MONTHLY NOTICES

OF THE

ROYAL ASTRONOMICAL SOCIETY

Vol. 99 No. 6

MEETING OF 1939 APRIL 14

Professor H. C. Plummer, President, in the Chair.

The election by the Council of the following Fellows was duly confirmed :—

Ibrahim Hilmy Abd-el-Rahman, B.Sc., Ornan Court, London, N.W. 3 ;
Akbar Ali, M.A., 15 Chatsworth Avenue, London, N.W. 4 ;
Pares-Chandra Chaudhuri, M.Sc., 54 Oakley Square, London, N.W. 1 ;
William Henry de Bargue Hubert, 44 Wimpole Street, London, W. 1 ;
William Jacob Jones, D.Sc., F.I.C., F.Inst.P., Professor of Chemistry, University College, Cardiff ;
Miss Eleanor Margaret Peachey, 115 Greenhill, Hampstead, London, N.W. 3 ; and
L. M. Verghese, B.Sc., Ornan Court, London, N.W. 3.

The following candidates were proposed for election as Fellows of the Society, the name of the proposers from personal knowledge being appended :—

Terence John Harding, 140 Ravenhurst Road, Harborne, Birmingham (proposed by J. R. Jeffreys) ; and
Noel Bryan Slater, Solar Physics Observatory, Cambridge (proposed by F. J. M. Stratton).

Eighty-three presents were announced as having been received since the last meeting, including :—

Royal Observatory, Edinburgh : Publications, Vol. I, No. 1.
Mount Wilson Observatory : Papers, Vol. 5, pts. 1 and 2. (Magnetic Observations of Sunspots, 1917–1924, by G. E. Hale and S. B. Nicholson.)

UNIVERSITY LIBRARY

The President announced that under the terms of the bequest of the late A. Stanley Williams the Society had recently come into the possession of the following instruments :—

$9\frac{1}{4}$-inch Calver reflector.
$6\frac{1}{2}$-inch reflector on equatorial mounting (which is at present not in perfect condition).
5-inch photographic lens.

Applications were invited for the loan of any of these instruments.

COLLISIONS AND THE THEORY OF RADIATIVE EQUILIBRIUM

R. v. d. R. Woolley

1. There are two methods of attempting to find out the behaviour of the outer layers of a star : one method is to assume a model, develop the properties of the model until we arrive at characteristics which can be compared with the observational characteristics of real stars ; and the other method is to make a microscopic analysis of the stellar atmosphere and attempt to determine the properties of the atmosphere from the properties of the constituent atoms and electrons. In particular, the theory of the radiative equilibrium of the outer layers of a star, due mostly to the researches of Professor Milne, which proceeds by making use of coefficients of absorption and laws representing certain types of equilibrium, may be justified either by developing certain assumptions and making comparisons with observation or by making an analysis of the atmosphere in terms of its constituent particles and attempting to establish the type of equilibrium thereby. Milne described two main types of equilibrium which he called local thermodynamic equilibrium and monochromatic radiative equilibrium. (They will be defined in paragraph 2.) He developed the theory of local thermodynamic equilibrium and obtained a satisfactory agreement with observation, and later he made a microscopic analysis in which he came to the conclusion that the atmosphere is substantially in local thermodynamic equilibrium beneath the surface, but that the type of equilibrium changes to monochromatic radiative equilibrium at the surface itself, the local thermodynamic equilibrium being set up by collisions which disappear at the surface. The present paper offers an alternative analysis of the effect of collisions which, being based on different ideas, arrives at a different conclusion from Milne's, namely, that local thermodynamic equilibrium persists right up to the surface. The paper also contains a solution of the mathematical problem presented by an atmosphere in which the type of equilibrium *does* change ; it is shown that some results are independent of the type of equilibrium, while the dependence of other results is shown explicitly. The present microscopic analysis is supported by an appeal to observation.

2. Let $I_\nu(\theta)d\nu d\omega/4\pi$ be the flow per sq. cm. per sec. of radiation in frequencies between ν and $\nu+d\nu$ travelling in a solid angle $d\omega$ at an angle θ to the vertical (the axis of x). Consider a cylinder of unit cross-section of length $ds=dx$ sec θ with its axis in the direction θ. Let ρ be the density of the atmosphere. The coefficient of absorption is k_ν if the amount of radiation absorbed in the cylinder per second from the flow $I_\nu(\theta)$ is

$$k_\nu \rho ds \,.\, I_\nu(\theta)d\nu d\omega/4\pi.$$

Further, let j_ν be the emission of energy per gramme per second, supposed isotropic so that $j_\nu d\omega/4\pi$ will go into the solid angle $d\omega$. Then the well-known equation for the transfer of radiation is

$$\frac{dI_\nu(\theta)}{\rho ds} = -k_\nu I_\nu(\theta)+j_\nu.$$

Milne defines the state of *local thermodynamic equilibrium* as the state in which the emission of radiation is the same as if the material were in full equilibrium at some temperature T, or

$$j_\nu = k_\nu B_\nu,$$

where $B_\nu=(2h\nu^2/c^2)\,(e^{h\nu/RT}-1)^{-1}$.

On the other hand, the material is said to be in *monochromatic radiative equilibrium* in respect of the ν radiation when it emits just as much as it absorbs, or

$$j_\nu = k_\nu \int I_\nu(\theta)\frac{d\omega}{4\pi} = k_\nu \mathfrak{J}_\nu.$$

Material in the outer layers of a star might be in one of these two types of equilibrium, or it might be in neither. We can test the hypothesis that the outer layers of a star are substantially in local thermodynamic equilibrium by developing the equations, finding the resulting spectral distribution of the emergent radiation and darkening to the limb, and comparing these results with observation, as Milne has done *; or we can examine the hypothesis by making a microscopic analysis of the material. The principle of detailed balancing has to be rejected, because the material is certainly not in unqualified thermodynamic equilibrium; but there is one condition that is still valid, namely, that the material at any point is in a steady state as regards the distribution of atoms among the stationary states. Milne has carried out the microscopic analysis in the case of an assembly of atoms supposed capable of two and only two stationary states. He arrived at the conclusion that in the absence of collisions such an assembly would be in monochromatic radiative equilibrium, but that with pressures such as may be expected in the photosphere collisions bring about a close approach to local thermodynamic equilibrium.†

3. We now examine the *three*-state problem, the three states considered being the ground state of the atom, a single excited state and the state of

* *Phil. Trans. R.S.*, **223**, 201, 1922.

† *M.N.*, **88**, 493, 1928.

ionization.* Let n_1, n_2 be the numbers of atoms per c.c. of the atmosphere in the ground state and in the excited state, and let $n(v)dv$ be the number of free electrons per c.c. of the atmosphere with velocities between v and $v+dv$. Further, let n_1^0, n_2^0, $n^0(v)dv$ be the corresponding numbers in thermodynamic equilibrium at some reference temperature T. (We shall not burden the notation by using a suffix T calling attention to this explicitly.) Further, let

$$n_1/n_1^\circ = t_1, \qquad n_2/n_2^\circ = t_2, \qquad n(v)/n^\circ(v) = t(v).$$

The number of upward transitions per c.c. per sec. from state h to state k is

$$n_h a_{hk} \cdot \frac{4\pi}{c}\mathcal{J}(\nu_{hk}), \qquad \text{written for short } t_h \,.\, (hk),$$

and the number of downward transitions per c.c. per sec. is

$$n_k\left\{b_{kh} + a_{kh} \cdot \frac{4\pi}{c} \cdot \mathcal{J}(\nu_{hk})\right\}, \qquad \text{written for short } t_k \,.\, (kh).$$

These statements define (hk) and (kh). Here b_{kh}, a_{kh} and a_{hk} are the Einstein transition coefficients as used by Eddington in *I.C.S.* (Milne adopts special definitions to get rid of the factor $4\pi/c$), so that

$$q_k b_{kh} = q_h a_{hk} 8\pi h c^{-3} \nu_{hk}^3, \qquad q_k a_{kh} = q_h a_{hk}.$$

Now suppose that the intensity $\mathcal{J}(\nu_{hk})$ is a certain fraction $w(\nu, \tau)$ of the intensity of equilibrium radiation $B(\nu_{hk})$ at the adopted reference temperature T.

Then

$$\frac{4\pi}{c}\mathcal{J}(\nu_{hk}) = w(\nu, \tau) \,.\, 8\pi h c^{-3} \nu_{hk}^3 (e^{h\nu/RT} - 1)^{-1}; \quad \text{also} \quad q_h n_k^0 = q_k n_h^0 e^{-h\nu_{hk}/RT}.$$

These relations give

$$\frac{(kh)}{(hk)} = \frac{1}{w(\nu, \tau)} + \left(1 - \frac{1}{w(\nu, \tau)}\right) e^{-h\nu/RT}.$$

The conditions that the numbers of particles per c.c. are steady are

$$\begin{array}{lll} -t_1\{\int(1v)dv + (12)\} & +t_2(21) & +\int t(v)(v1)dv = 0, \\ t_1(12) & -t_2\{\int(2v)dv + (21)\} & +\int t(v)(v2)dv = 0, \\ t_1(1v) & +t_2(2v) - t(v)\{(v1) + (v2)\} & = 0, \end{array}$$

the third row being representative of an infinite set of such equations, one for each v. Considering all the v's together for the moment as a single state the equations reduce to three and the explicit solutions are

$$\frac{t_2}{t_1} = \frac{(12)(v1) + (12)(v2) + (1v)(v2)}{(21)(v1) + (21)(v2) + (v1)(2v)},$$

$$\frac{t_v}{t_1} = \frac{(21)(1v) + (12)(2v) + (1v)(2v)}{(21)(v1) + (21)(v2) + (v1)(2v)}.$$

* The particular results obtained from the three-state problem are a guide to the general problem: the microscopic theory of a stellar atmosphere is really the n-state problem.

In thermodynamic equilibrium $w(\nu, \tau) = 1$ everywhere so that all $(hk) = (kh)$, but at the outside of a star this is not so. The simplest kind of departure is *geometrical dilution* of the radiation such as is the case outside a body radiating like a black body, when $w(\nu) = W$ equal to the solid angle subtended at the point considered: in particular on the surface of a star radiating like a black body $w(\nu) = \frac{1}{2}$ for all ν. This geometrical dilution is a standard case which we shall examine.

Pannekoek has published a table of values of (hk) for the hydrogen spectrum under solar conditions. Let us consider the three states $1S$, $2P$ and ionization (state 5 in Pannekoek's notation). The logarithms to base 10 of the pairs of quantities which occur are

$(21)(v1)$	$(21)(v2)$	$(v1)(v2)$
8·79	7·69	5·20

from which it is clear that a very good approximation to the state of affairs is

$$t_2/t_1 = t_v/t_1 = W$$

under geometrical damping. Further, to this order of approximation $t_1 \,.\, (12) = t_2 \,.\, (21)$ and $t_1 \,.\, (1v) = t_v \,.\, (v1)$ so that the atmosphere is very nearly in monochromatic radiative equilibrium so far as these frequencies are concerned. On the other hand $t_v \,.\, (v2) = W^{-1} t_2 (2v)$ and the atmosphere is strongly fluorescent in this frequency, monochromatic radiative equilibrium being here upset.

We now turn to collisions. Collisions affect the v-distribution and tend to redistribute the electron velocities according to a Maxwellian scheme. Since full thermodynamic equilibrium gives a Maxwellian electron velocity distribution, an externally imposed Maxwellian velocity distribution means that the emission of continuous radiation (which can only depend on fixed capture probabilities and on the electron velocity distribution) must be precisely the same as if the material were in strict thermodynamic equilibrium at *some* temperature T, or

$$j_\nu = (k_\nu)_T B(\nu, T),$$

the suffix T to k_ν is necessary because k_ν, the coefficient of absorption actually encountered by the radiation, is not necessarily the same as the coefficient for thermodynamic equilibrium since it depends on the populations of the secondary states.* It must be noticed, however, that *very* abundant collisions (especially superelastic and inelastic collisions) will tend to arrange these populations in the same Maxwellian scheme as the electron velocities, so that the type of equilibrium must tend to local thermodynamic equilibrium as the pressure increases. We shall show later in this section, however, that we do not have to appeal to superelastic and inelastic collisions to wipe out the distinction between k_ν and $(k_\nu)_T$.

At first sight we might suppose that fluorescence is very important so far as the visible spectrum is concerned, because the continuous spectra forming k_ν in the visible region must spring from subordinate states, visible

* I owe this remark to Dr. Krook.

light having too low a frequency to ionize an atom from its ground state. It is likely, however, that fluorescence is very much a skin effect and that the dilution dies away very rapidly beneath the surface. It is not possible to calculate $w(\nu, \tau)$ satisfactorily from existing theory because, as is well known, theoretical curves for the spectral energy distribution do not fit the observed (Abbott's) curve, so that a theoretical calculation of $w(\nu, \tau)$ may be misleading. However, we may quote a well-known result from the theory of radiative equilibrium (eq. 4.6 *infra*).

$$\mathcal{J}_\nu = B_\nu + \frac{2b_\nu - 3a_\nu}{3+2\sqrt{3}} e^{-\tau_\nu \sqrt{3}},$$

where $B_\nu = a_\nu + b_\nu \tau_\nu$. From this result it follows that as τ_ν increases $\mathcal{J}_\nu \to B_\nu$ or $w_\nu \to 1$. Now the existence of geometrical dilution at the surface arises since b_ν/a_ν increases with ν so that $\mathcal{J}_\nu < B_\nu$ in the infra-red and $\mathcal{J}_\nu > B_\nu$ in the ultra-violet. Following Krook * we may suppose that τ_ν increases very strongly in the ultra-violet ; if this is so, the ultra-violet excess of $\mathcal{J}_\nu$ over B_ν will be effectively wiped out at quite small optical depths judging the optical depth in the visible region. On this account we shall suppose in the remainder of this paper that fluorescence is negligible.

The difference between k_ν and $(k_\nu)_T$ depends on the populations of the stationary states, and these will in turn depend on the values of $\mathcal{J}$ appropriate to the frequencies connecting these states to the ground state or to some lower state : in either case they are line frequencies. Now for a line frequency

$$\mathcal{J}_\nu = B_\nu + \frac{\frac{2}{3}b_\nu - a_\nu(1+\eta_\nu)}{1+\eta_\nu+\frac{2}{3}q_\nu} e^{-q_\nu \tau_\nu},$$

where η_ν is the ratio of line absorption to continuous absorption and is a large number in the centre of the line, and $q_\nu^2 = 3(1+\eta_\nu)$ so that q_ν is also a large number. It follows that the recovery of $\mathcal{J}_\nu$ to B_ν takes place much nearer the surface $\tau_\nu = 0$ for line frequencies than for other frequencies. For this reason the stationary states will have populations appropriate to $B(T)$ everywhere except very near the surface : in other words, $k_\nu = (k_\nu)_T$ except for a very thin layer (judged by τ_ν) near the surface. In the remainder of this paper we shall ignore the distinction between k_ν and $(k_\nu)_T$. We now have to establish the form of j_ν, the energy emitted per gramme per second, when collisions establish a mixture of the two types of equilibrium. To simplify the argument, suppose that there is only one kind of atom present, so that the absorption of a quantum in the frequency range ν to $\nu + d\nu$ corresponds to the liberation of a free electron with a velocity in the particular range v to $v + dv$. (Our result does not depend on this restriction.) In time dt one gramme of matter absorbs the amount of energy $k_\nu \mathcal{J}_\nu d\nu dt$ in the frequency range considered from a radiation field $\mathcal{J}_\nu$. The number of quanta absorbed is $(h\nu)^{-1} k_\nu \mathcal{J}_\nu d\nu dt$. Let $F_0(v)dv$ be the number of electrons set free per gramme per second with velocities between v and $v + dv$: then

$$(h\nu)^{-1} k_\nu \mathcal{J}_\nu d\nu = F_0(v)dv. \qquad (3.1)$$

* *M.N.*, 98, 204, 1938.

If the radiation is temperature radiation, *i.e.* $\mathcal{J}_\nu = B_\nu$, the velocity distribution is Maxwellian and we have

$$(h\nu)^{-1}k_\nu B_\nu d\nu = M(v)dv. \tag{3.2}$$

Let $\int F_0(v)dv = N$. Consider the history of $N\Delta t$ electrons set free in the time interval $t = 0$ to $t = \Delta t$ (as a result of the absorption $\Delta t \int k_\nu \mathcal{J}_\nu d\nu$). If the electrons are unable to recombine collisions will gradually alter the velocity distribution from $F_0(v)$ to $M(v)$. Let $F(v)$ be the distribution at time t. Then we may suppose that

$$F(v) - M(v) = (F_0(v) - M(v))e^{-\lambda t},$$

where λ^{-1} is the "time of relaxation" similar to the time of relaxation for restoring spherical symmetry.* But on account of recombinations during any time interval dt a fraction μ of the electrons will be removed, and at time t the number of electrons, set free at $t = 0$, having velocities between v and $v + dv$ at time t, and recombining between t and $t + dt$ is

$$\Delta t \mu e^{-\mu t}\{M(v) + (F_0(v) - M(v))e^{-\lambda t}\}dvdt.$$

The time integral of this expression

$$\Delta t\left[\frac{\mu}{\lambda+\mu}F_0(v)dv + \frac{\lambda}{\lambda+\mu}M(v)dv\right] \tag{3.3}$$

is the number of recombinations in the velocity range v to $v + dv$ arising from the $N\Delta t$ electrons. It is also the number of quanta emitted in the range ν to $\nu + \Delta\nu$, and the energy emitted per gramme per second in this frequency range is $j_\nu d\nu$, where

$$j_\nu = \frac{\mu}{\lambda+\mu}k_\nu \mathcal{J}_\nu + \frac{\lambda}{\lambda+\mu}k_\nu B_\nu \tag{3.4}$$

from (3.3), using equations (3.1) and (3.2).

The values of λ and μ depend upon the probability that a particular electron will encounter another electron and the probability that it will be captured by an ion respectively. To get some idea of the relative probabilities, let us consider a gas having two types of molecules each having a Maxwellian velocity distribution appropriate to a temperature T. The number of collisions per c.c. per sec. between molecules of types p and q is

$$2\nu_p\nu_q S_{pq}{}^2\sqrt{2\pi RT\left(\frac{1}{m_p}+\frac{1}{m_q}\right)},$$

where ν_p, ν_q, m_p, m_q are the numbers of molecules per c.c. and the masses of the two types of molecule respectively, and S_{pq} is the sum of the radii of types p and q. From this equation it is clear that since the mass of the electron is much smaller than the mass of an ion, and since there must be at least as many electrons per c.c. as ions, collisions between electrons must be much more frequent than captures of electrons by ions unless the target for electron capture is much greater than the target for electron collisions.

* Jeans, *Dynamical Theory of Gases* (2nd Edition), p. 260.

Actually it is much smaller. From Eddington's *Internal Constitution of the Stars*, § 154, the radius σ_1 of the target for the capture of electrons with velocity v by singly charged ions is

$$\sigma_1 = (4\pi)^{1/5} \frac{e^2}{mv^2} \left(\frac{v}{c}\right)^{3/5},$$

while (p. 278) the apparent target σ_2 for a 90° deflection between two electrons each with velocity v is

$$\sigma_2 = \frac{1}{4} \frac{e^2}{mv^2},$$

so that for all practical values of v/c, $\sigma_2 >> \sigma_1$. It is clear that even if quite a large number of electron collisions are required to establish e^{-1} relaxation (and judging by Jeans' figures for the relaxation of unsymmetrical motions, only about two are required) $\lambda >> \mu$ and *local thermodynamic equilibrium is always substantially maintained by electron collisions whatever the electron pressure so far as continuous absorption and emission is concerned.* Milne's analysis * refers to line processes as affected by superelastic and inelastic collisions, and shows that so far as they are concerned local thermodynamic equilibrium gives way to monochromatic radiative equilibrium in the absence of collisions: the population of his upper state relative to the lower state is controlled by the radiation in the absence of collisions. But if the continuous absorption arises from a bound-free transition, the population of the upper state itself creates the electron pressure, and the case is quite different from Milne's. The only escape from our conclusion—that the equilibrium is necessarily local thermodynamic equilibrium—is the possibility that some of the continuous absorption (radiation "between the lines") arises from bound-bound transitions (in the wings of strong lines, in very weak lines, or perhaps in lines broadened by Stark effect). If the contributions to k_ν "between the lines" on these accounts are substantial, Milne's original conclusion—a change-over from monochromatic to local thermodynamical equilibrium with increasing depth—is partly restored.

4. We now turn to the effect of the type of equilibrium on the observable properties of the star. Certain results follow from the form of equation (3.4) (which is essentially the same as that found by Milne †) without a knowledge of λ and μ and their variation with τ (provided that λ does not vanish). Let $\lambda/(\lambda+\mu) = \epsilon$. Then the equation of transfer of radiation of frequency ν is

$$\cos\theta \frac{dI_\nu(\theta)}{\rho dx} = -k_\nu I_\nu(\theta) + \epsilon k_\nu B_\nu + (1-\epsilon) k_\nu \mathcal{J}_\nu.$$

First suppose that $k_\nu = k$, independent of ν. Introducing the optical depth τ defined by $\tau = \int_x^0 k\rho dx$ we get

$$\cos\theta \frac{dI_\nu(\theta)}{d\tau} = I_\nu(\theta) - \epsilon B_\nu - (1-\epsilon)\mathcal{J}_\nu.$$

* *M.N.*, **88**, 493, 1928.

† *M.N.*, **88**, 498 (eq. 24), 1928.

Multiply this equation by $d\nu$ and integrate. We get

$$\cos\theta\frac{dI(\theta)}{d\tau}=I(\theta)-\epsilon B-(1-\epsilon)\mathcal{J},$$

where $I(\theta)=\int I_\nu(\theta)d\nu$, etc. Treating this equation in the usual way we first multiply by $d\omega$ and integrate over a sphere; then multiply the original equation by $d\omega\cos\theta$ and integrate over a sphere, getting

$$\frac{dH}{d\tau}=\epsilon(\mathcal{J}-B),$$

$$\frac{dK}{d\tau}=H,$$

where

$$H=\int I(\theta)\cos\theta d\omega/4\pi, \qquad K=\int I(\theta)\cos^2\theta d\omega/4\pi.$$

H is the outward flow of radiation per sq. cm. per second, integrated over all frequencies and is constant in the outer layers of a star, where there is no generation of energy, so that $dH/d\tau=0$. Then *so long as* ϵ *is not zero* $\mathcal{J}=B$. If we use the well-known first approximation to the θ-distribution of $I(\theta)$ and set $K=\frac{1}{3}\mathcal{J}$ we get the familiar result

$$B=\mathcal{J}=3H\tau+\text{const.}$$

Introducing the boundary condition appropriate to the first approximation for θ, viz. $\mathcal{J}=2H$ at $\tau=0$,

$$B=\mathcal{J}=H(2+3\tau)$$

and since B is proportional to T^4 we get the well-known Milne equation for the temperature distribution,

$$T^4=T_0^4(1+\tfrac{3}{2}\tau),$$

here shown to be true not only in the case of local thermodynamical equilibrium but also in the case of a mixture of local thermodynamic equilibrium and monochromatic radiative equilibrium *provided that* ϵ *does not vanish* right up to the boundary $\tau=0$.

We now return to the spectral distribution of the radiation. We shall not distinguish between $(k_\nu)_T$ and k_ν, but we abandon the restriction that k_ν is independent of ν. The equation of transfer gives

$$\frac{dH_\nu}{d\tau_\nu}=\epsilon(\mathcal{J}_\nu-B_\nu), \tag{4.1}$$

$$\frac{dK_\nu}{d\tau_\nu}=H_\nu. \tag{4.2}$$

While H is independent of τ, H_ν is not. The outer layers cannot generate energy, but they can and do transfer it from one frequency to another. To get back to H we define a mean coefficient of absorption $\bar{k}$ by

$$\bar{k}=\frac{1}{H}\int k_\nu H_\nu d\nu \tag{4.3}$$

and let $\bar{\tau} = \int_x^0 \bar{k}\rho dx$. Then $Hd\bar{\tau} = \int_\nu H_\nu d\tau_\nu d\nu$, so that integrating equation (4.2) with respect to ν we get

$$\frac{dK}{d\bar{\tau}} = H.$$

Then proceeding as before we get

$$\mathcal{J} = H(2 + 3\bar{\tau}). \tag{4.4}$$

The equation no longer leads directly to a temperature distribution since we no longer have $B = \mathcal{J}$, the relation being $\int k_\nu B_\nu d\nu = \int k_\nu \mathcal{J}_\nu d\nu$. Equations (4.1) and (4.2) may be combined together by using $K_\nu = \frac{1}{3}\mathcal{J}_\nu$, which gives

$$\frac{d^2\mathcal{J}_\nu}{d\tau_\nu^2} = 3\epsilon(\mathcal{J}_\nu - B_\nu).$$

To solve this equation we suppose that a sufficient approximation to the variation of B_ν with τ_ν is $B_\nu = a_\nu + b_\nu\tau_\nu$; then

$$\frac{d^2}{d\tau_\nu^2}(\mathcal{J}_\nu - B_\nu) = 3\epsilon(\mathcal{J}_\nu - B_\nu), \tag{4.5}$$

with $\epsilon = 1$ equation (4.5) is the well-known equation for local thermodynamic equilibrium.

The well-known solution of equation (4.5) in this case is

$$\mathcal{J}_\nu = a_\nu + b_\nu\tau_\nu + \frac{2b_\nu - 3a_\nu}{3 + 2\sqrt{3}} e^{-\tau_\nu\sqrt{3}}. \tag{4.6}$$

We must suppose that we are given a value of T_0 corresponding to a knowledge of the solar constant. This determines a_ν since $a_\nu = B(\nu, T_0)$. The values of b_ν are implicit in the result (4.4); they correspond to a knowledge of the temperature *gradient* near the surface. We might for example adopt a trial value of the temperature gradient and compute the values of b_ν from it. We then have $\mathcal{J}_\nu$ from (4.6) and if our choice of gradient is correct integrating (4.6) with respect to ν will reproduce (4.4).

A case of especial interest is that in which k_ν is constant with ν except for the presence of absorption lines. If these lines are either equally spaced or distributed at random, the relation $\mathcal{J} = B$ is preserved so that the temperature distribution is given by

$$T^4 = T_0^4(1 + \tfrac{3}{2}\bar{\tau}). \tag{4.7}$$

Further, $k_\nu = \beta\bar{k}$, $\tau_\nu = \beta\bar{\tau}$ where β is a quantity less than unity whose value will depend on the number and strength of the absorption lines present (it will be evaluated by (4.3)). Then, writing α for $h\nu/RT$ we have

$$a_\nu = B(\nu, \tau_0), \qquad b_\nu = a_\nu(1 - e^{-\alpha})^{-1} \cdot \frac{3\alpha}{8\beta}. \tag{4.8}$$

These values inserted in (4.6) give a complete account of $\mathcal{J}_\nu$. But of course equation (4.5) cannot be solved unless we know ϵ as a function of τ_ν. A solution for a special case is given in the next section.

5. The essential feature in Milne's view of ϵ is that it is very small when τ or $\tau_\nu = 0$ (since the pressure vanishes at the surface of the star) and tends to the limit 1 as τ attains large values. Hence a suitable representation of this variation is

$$\epsilon = 1 - e^{-\gamma\tau} = 1 - e^{-\gamma_\nu \tau_\nu}. \tag{5.1}$$

The form (5.1) must be regarded as a suitable interpolation formula which is at least an improvement on the pioneer device of fitting an atmosphere in which $\epsilon = 0$ to an atmosphere in which $\epsilon = 1$. The equation (4.5) becomes

$$\frac{d^2}{d\tau_\nu{}^2}(\mathcal{J}_\nu - B_\nu) = 3(1 - e^{-\gamma_\nu\tau_\nu})(\mathcal{J}_\nu - B_\nu). \tag{5.2}$$

Write y_ν for $(\mathcal{J}_\nu - B_\nu)$ and let $z_\nu = \gamma_\nu{}^{-1} \cdot 2\sqrt{3}e^{-\frac{1}{2}\gamma_\nu\tau_\nu}$ and $n_\nu = \lambda_\nu{}^{-1} \cdot 2\sqrt{3}$. Equation (5.2) becomes

$$z^2\frac{d^2y}{dz^2} + z\frac{dy}{dz} + y(z^2 - n^2) = 0 \tag{5.3}$$

(omitting all suffixes ν). This is Bessel's equation of order n. If n is an integer the solution is

$$y = P_\nu \mathrm{J}_n(z) + Q_\nu \mathrm{Y}_n(z), \tag{5.4}$$

where P_ν and Q_ν are arbitrary constants. The boundary condition at $\tau_\nu = \infty$ (which is $z = 0$) gives $Q_\nu = 0$ since $\mathrm{Y}_n(0) = \infty$ and y must remain finite. Restoring $\mathcal{J}_\nu - B_\nu$ for y we have

$$\mathcal{J}_\nu - B_\nu = P_\nu \mathrm{J}_n(z) \tag{5.5}$$

with the further boundary condition that $\mathcal{J}_\nu = 2H_\nu$ at $\tau_\nu = 0$, *i.e.* at $z = \gamma^{-1} \cdot 2\sqrt{3} = n$. Since $H_\nu = \frac{1}{3}\frac{d\mathcal{J}_\nu}{d\tau_\nu}$ this condition gives

$$P_\nu\left\{\mathrm{J}_n(n) + \frac{2}{\sqrt{3}}\mathrm{J}_n{}'(n)\right\} = \tfrac{2}{3}b_\nu - a_\nu, \tag{5.6}$$

and the explicit solution for $\mathcal{J}_\nu$ is accordingly

$$\mathcal{J}_\nu = a_\nu + b_\nu\tau_\nu + \frac{(2b_\nu - 3a_\nu)\mathrm{J}_n(z)}{3\mathrm{J}_n(n) + 2\sqrt{3}\mathrm{J}_n{}'(n)}. \tag{5.7}$$

This equation is analogous to (4.6) and the same remarks as were made in paragraph 4 apply to a_ν and b_ν.

In the special case where k_ν is constant with ν except for absorption lines equation (4.7) stands and a_ν and b_ν are given by (4.8). Further n_ν does not vary with ν.

In comparing any theory of the radiative equilibrium of the star with observation, we are concerned with the emergent radiation in monochromatic light, namely

$$I_\nu(0, \theta) = \int_0^\infty j_\nu \rho dx \sec\theta \; e^{-k\rho x \sec\theta} \tag{5.8}$$

(in which x is measured positive downwards). For local thermodynamical equilibrium $j_\nu = k_\nu B_\nu$ and the efflux is

$$I_\nu(0, \theta) = \int_0^\infty B_\nu(\tau_\nu) d\tau_\nu \sec\theta \; e^{-\tau_\nu \sec\theta}.$$

We shall consider the special case in which τ_ν is constant with ν except for the absorption lines so that $\tau_\nu = \beta\bar{\tau}$. Then

$$T^4 = T_0^4(1 + \tfrac{3}{2}\bar{\tau}) \quad \text{and} \quad T = T_0\left(1 + \frac{3}{2\beta}T_\nu\right).$$

Taking as independent variable $x = \tau_\nu \sec\theta$ we have

$$T = T_0\left(1 + \frac{3}{2\beta}x\cos\theta\right)$$

and we get

$$I_\nu(0, \theta) = \frac{2h\nu^3}{c^2}\int_0^\infty \frac{e^{-x}dx}{e^{h\nu/RT_0\left(1+\frac{3}{2\beta}x\cos\theta\right)^{-\frac{1}{4}}} - 1} \tag{5.9}$$

$$= \frac{2h\nu^3}{c^3}\alpha^{-5}f(\alpha, p), \tag{5.10}$$

where $f(\alpha, p)$ is the function described by Milne *

$$f(\alpha, p) = \alpha^5\int_0^\infty \frac{e^{-x}dx}{e^{\alpha(1+px)^{-\frac{1}{4}}} - 1}.$$

In our case

$$\alpha = h\nu/RT_0 \quad \text{and} \quad p = \frac{3}{2\beta}\cos\theta.$$

Bringing in the term representing monochromatic radiative equilibrium we have

$$\begin{aligned} j_\nu = k_\nu(\epsilon B_\nu + (1-\epsilon)\mathcal{J}_\nu) &= k_\nu\{\epsilon B_\nu + (1-\epsilon)(B_\nu + P_\nu \mathrm{J}_n(z))\} \\ &= k_\nu\{B_\nu + e^{-\gamma_\nu\tau_\nu}P_\nu \mathrm{J}_n(z)\}. \end{aligned} \tag{5.11}$$

Now $\mathrm{J}_n(z)$ is positive if $z < n$, so that the excess or defect of j_ν over $k_\nu B_\nu$ depends on the sign of P_ν which is the sign of $\frac{2}{3}b_\nu - a_\nu$. With the values of b_ν and a_ν given by (4.8) we see that $\frac{2}{3}b_\nu - a_\nu$ changes sign from negative to positive as we go from the infra-red to the ultra-violet. We can say at once that *the introduction of monochromatic radiative equilibrium gives more violet light compared with red*, i.e. *a higher colour temperature* which is an expected result since the introduction of monochromatic radiative equilibrium brings in some $\mathcal{J}_\nu$ instead of B_ν, and $\mathcal{J}_\nu$ is richer in high frequencies than B_ν.

It is worth noticing that with the values (4.8)

$$\int_0^\infty (2b_\nu - 3a_\nu)d\nu = 0, \quad \text{so that} \quad \int_0^\infty P_\nu d\nu = 0.$$

This checks our result in paragraph 4 that $\mathcal{J} = B$, *i.e.* $\int\mathcal{J}_\nu d\nu = \int B_\nu d\nu$.

* *Phil. Trans. R.S.*, **223**, 201, 1922.

Using (5.8) and (5.11) the emergent radiation is given by

$$I_\nu(0, \theta) = \int_0^\infty \{B_\nu(\tau)e^{-\tau_\nu \sec\theta} + P_\nu \mathrm{J}_n(z)e^{-(\gamma_\nu + \sec\theta)\tau_\nu}\} \sec\theta \, d\tau_\nu. \quad (5.12)$$

The first term is the familiar Milne integral. To evaluate the second let $m = 2 \sec\theta/\gamma_\nu$. Since $z = ne^{-\frac{1}{2}\gamma_\nu\tau_\nu}$ we have

$$e^{-(\gamma_\nu + \sec\theta)\tau_\nu} \sec\theta \, d\tau_\nu = -mn^{-(2+m)}z^{1+m}dz.$$

Then

$$\int_0^\infty P_\nu \mathrm{J}_n(z)e^{-(\gamma_\nu + \sec\theta)\tau_\nu} \sec\theta \, d\tau_\nu = P_\nu mn^{-(2+m)}\int_0^n \mathrm{J}_n(z)z^{1+m}dz.$$

Let

$$n^{-(2+m)}\int_0^n \mathrm{J}_n(z)z^{1+m}dz = \Phi_n(m).$$

But *

$$\mathrm{J}_n(z) = \frac{z^n}{2^n \cdot n!}\{1 - A_1z^2 + A_2z^4 - A_3z^6 \ldots\},$$

where

$$A_p = (4^p \cdot p! \; 4 \cdot 5 \cdot 6 \ldots (3+p))^{-1}.$$

Hence integrating term by term

$$\Phi_n(m) = \frac{n^n}{2^n n!}\left\{\frac{1}{m+n+2} - \frac{A_1n^2}{m+n+4} + \frac{A_2n^4}{m+n+6} \ldots\right\}. \quad (5.13)$$

The series is rapidly convergent. For a given n, a table of values of $\Phi_n(m)$ may be constructed easily by computing values of A_1n^2, A_2n^4, etc., once and for all and multiplying these values by the appropriate denominators for different values of m.

P_ν is given by (5.6) and b_ν and a_ν are given by (4.8). With the notation $\alpha = h\nu/RT_0$ we have

$$P_\nu = \frac{B(\nu, T_0)}{\mathrm{J}_n(n) + \frac{2}{\sqrt{3}}\mathrm{J}'_n(n)}\{\tfrac{1}{4}\alpha(1 - e^{-\alpha})^{-1} - 1\}.$$

Collecting the results together we have

$$I_\nu(0, \theta) \times \frac{c^2}{2h\nu^3} = \alpha^{-5}f(\alpha, p) + \frac{m\Phi_n(m)}{\mathrm{J}_n(n) + \frac{2}{\sqrt{3}}\mathrm{J}'_n(n)} \cdot (e^\alpha - 1)^{-1}\{\tfrac{1}{4}\alpha(1 - e^{-\alpha})^{-1} - 1\}. \quad (5.14)$$

This equation specifies the emergent radiation in all frequencies from centre to limb, the latter because both p and m depend on the angle of emergence θ.

To get an idea of the quantities involved, we may take $\beta = 1$ (*i.e.* disregard the absorption lines)† and take as our estimate of n Milne's datum that the

* Watson, *Theory of Bessel Functions*, p. 16.

† The absorption lines are omitted at this point to avoid a discussion of the value of β and also to avoid interpolation among Milne's values of $f(\alpha, p)$.

contribution to j_ν from the two types of equilibrium are about equal at $P_e = 10^{-4}$ atmospheres which we place at about $\tau = 0{\cdot}7$. The nearest integral value of n is 3. The value of $\left\{4(J_n(n) + \frac{2}{\sqrt{3}}J'_n(n))\right\}^{-1}$ is 0·4869, so that

$$P_\nu = 0{\cdot}4869 B(\nu, T_0)\{\alpha(1 - e^{-\alpha})^{-1} - 4\}.$$

Where there are no absorption lines $p = \frac{3}{2}\cos\theta$ and we have

$$I_\nu(0, \theta) \propto \alpha^{-2} f(\alpha, \tfrac{3}{2}\cos\theta) + 0{\cdot}4869\alpha^3(e^\alpha - 1)^{-1}\{\alpha(1 - e^{-\alpha})^{-1} - 4\} m\Phi_3(m). \quad (5.15)$$

Values of $\Phi_3(m)$ and $m\Phi_3(m)$ for various values of m, and the corresponding values of θ, are given in Table I.

TABLE I

$$\Phi_3(m) = 3^{-(m+2)} \int_0^3 J_3(z) z^{1+m} dz$$

Sec θ	m	$\Phi_3(m)$	$m\Phi_3(m)$
1·000	2·309	0·04864	0·11232
1·299	3	·04402	0·13203
1·732	4	·03866	0·15463
3·000	6·928	·02845	0·19709
4·763	11	·02076	0·22838

Milne * gives tables of values of $f(\alpha, 0{\cdot}5)$ and $f(\alpha, 1{\cdot}5)$ corresponding to sec $\theta = 3$ and sec $\theta = 1$ in our case. Table II shows numbers proportional to $I_\nu(0, \theta)$ computed from (5.15) for sec $\theta = 1$ and sec $\theta = 3$ using the values of α listed directly by Milne and his value of T_0, namely 4830°.

TABLE II

Emergent Radiation from (5.15)

Wave-lengths in A.	Sec $\theta = 1$				Sec $\theta = 3$				
	7862	5897	4717	3931	8933	6700	5360	4717	4466
α	3·772	5·030	6·287	7·545	3·320	4·427	5·533	6·287	6·640
$\alpha^{-2}f(\alpha, p)$	2·679	2·297	1·683	1·118	1·888	1·599	1·156	0·858	0·739
Second term	−0·009	+0·049	+0·058	+0·044	−0·073	+0·049	+0·101	+0·102	+0·097
Sum	2·670	2·346	1·741	1·162	1·815	1·648	1·257	0·960	0·836

The value of $f(\alpha, 0{\cdot}5)$ for $\alpha = 6{\cdot}287$ was found by interpolation among Milne's values.

Consider first the values for sec $\theta = 1$, the centre of the disc. Neither the set $\alpha^{-2}f(\alpha, p)$ nor the final sum is exactly a black-body distribution, but the figures correspond roughly to colour temperatures at the centre of the disc of 6250° and 6350° respectively. The effect of absorption lines is to raise the colour temperature by about a hundred and fifty degrees, so that either result is a little low on Plaskett's observed value of about 6850°. This

* *Phil. Trans. R.S.*, **223**, 247–8, 1922.

indicates that k_ν increases slightly from violet to red and as we have no *a priori* reason for supposing k_ν to be constant with ν, nothing more can be said in favour of one or the other.

When, however, we compare the two values of sec θ shown we see that the darkening to the limb is affected by the second term in (5.15). Milne obtained a 1 per cent. agreement between $\alpha^{-2}f(\alpha, p)$ and Abbott's observed values, and the second term in (5.15) spoils this, as is shown by Table III. (Abbott's values are taken by interpolation among figures quoted by Milne.)

TABLE III

Darkening to the Limb at 4717 A.

	Sec $\theta = 1$	Sec $\theta = 3$
Observed (Abbott)	1000	505
Local thermodynamic equilibrium	1000	510
(5.15)	1000	550

Table III is based on k_ν constant with ν, and the decrease of k_ν with ν suggested by the colour temperature makes matters worse for equation (5.15). (Since $p = \frac{3}{2} \cos\theta \frac{\bar{\tau}}{\tau_\nu}$ the fact that τ_ν is below the average decreases the value of cos θ corresponding to $p = 1{\cdot}5$, so that the predicted darkening now refers to a point nearer the limb, where it should be still lower.)

As Plaskett has shown, an exhaustive analysis of the significance of observations of darkening to the limb ought to include a discussion of convection. Such an analysis should perhaps be deferred until definitive measures of darkening to the limb have been secured. Nevertheless it seems clear that the data at present available suggest that the departure from local thermodynamic equilibrium towards monochromatic radiative equilibrium is very small, in agreement with the conclusion of our microscopic analysis in paragraph 3.

Summary.—The paper discusses the effect of collisions between electrons on the type of radiative equilibrium to be expected in the outer layers of a star and arrives at the conclusion that local thermodynamic equilibrium is substantially maintained by them. It is shown by developing the theory of a gradual change from local thermodynamic equilibrium to monochromatic radiative equilibrium and comparing the results with Abbott's observations of darkening to the limb that the terms representing monochromatic radiative equilibrium must be small, in agreement with the microscopic analysis.

ON THE INTENSITY OF *Mg* 5183 IN K-TYPE STARS

A. D. Thackeray

During the course of a spectrophotometric programme on line-intensities in K stars a well-marked variation of the line *Mg* 5183 with surface gravity has been detected which does not appear to have been remarked upon previously. Since the phenomenon has an important bearing upon the theory of absorption lines, it has been considered worth while to publish the result prior to completion of the programme, which is not primarily concerned with the study of absolute magnitude effects.

Observational Material.—All plates used in the present paper were taken with one instrument—the two-prism spectrograph attached to the Newall 25-inch refractor, giving a dispersion of 51 A./mm. at 5180 A. Most stars were taken on Ilford Hypersensitive Panchromatic plates and uniformly broadened to a width of 0·5 mm., thus avoiding difficulties of photographic grain; a few of the brightest stars were taken on Ilford Special Rapid Panchromatic plates. Photometric calibration was obtained by means of a step-slit spectrograph, characteristic curves being drawn for wave-lengths 5900 A., 5200 A. and $H\beta$; in the majority of plates it was found possible to draw a single characteristic curve for all three wave-lengths (although there is a rapid change in contrast to the blue side of $H\beta$, while some showed an appreciable increase in contrast to the red). The usual photometric precautions of brush development, exposure time of calibration, etc. were taken. The reductions to equivalent widths were made from tracings obtained with the Cambridge microphotometer in the normal manner. Interagreement between duplicate plates of the same star indicates a probable error in equivalent width of $\pm$ 7 per cent. Duplicate measures of *Mg* 5183 in 34 stars of type G5 to K6 are available, with single measures of 7 additional stars.

Difficulties due to blends and the drawing-in of the continuous spectrum are minimized in this particular programme owing to the following considerations: (1) Since only G5 to K5 stars are used here, blends will tend to affect measures in all stars to the same degree; (2) in the visual region the comparative paucity of lines eases the problem of the continuous spectrum, except for types K5 and later in which *TiO* bands begin to appear; (3) the line *Mg* 5183 is a particularly good line for measurement, as it is much stronger than any of its nearest neighbours in the spectrum. In evidence of the latter point we quote all lines listed by Hacker * in the spectrum of Arcturus (*g*K0) within 4 A. of *Mg* 5183 from measures of high-dispersion plates. Identifications in brackets are due to D. N. Davis.†

* *Princeton Contributions*, No. 16, 1935.
† *Ap. J.*, **86**, 109, 1937.

λ	Int.	Element
5180·05	4	*Fe*, (*MgH*)
80·54	3	(*TiO*, *MgH*)
83·92	30*W*	*Mg*
85·05?	2	⊙, (*MgH*)
85·91	7	Ti^{+}
86·45	5*n*	*Ti*, *Ni*
5187·54	1	...

Finally, special care has been devoted to rendering the material as homogeneous as possible, and one may conclude that any variation in intensity exceeding 15 per cent. such as has been observed may be attributed with confidence to real variations in intensity of the line *Mg* 5183.

Results.—In fig. 1 equivalent widths of *Mg* 5183 are plotted against spectral type. We have used the mean of Mount Wilson * and Victoria †

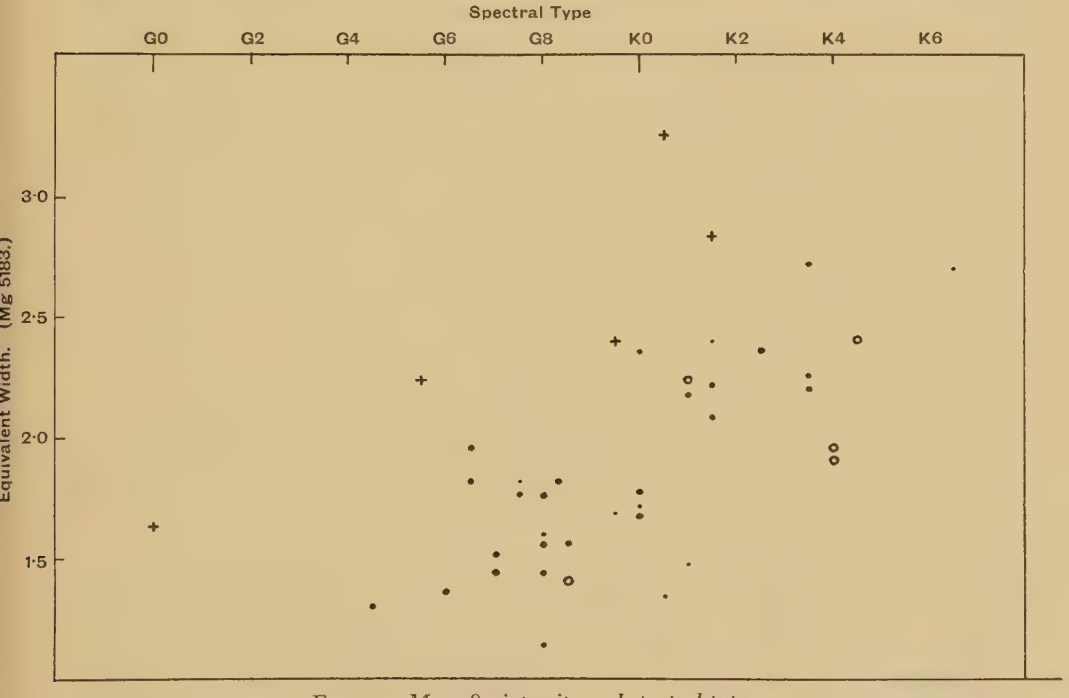

Fig. 1.—*Mg* 5183 *intensity and spectral type.*

+ dwarfs. ● giants. ○ supergiants.

types since they are more closely correlated with our measured intensities of other lines (*Fe*, *Na*, *Cr*) in the visual region than any other available types; since types are usually estimated on the basis of line-intensities in the photographic region, such a correlation may be regarded as a satisfactory index of the accuracy of spectral types. It will be noticed that *Mg* 5183 is abnormally strong in the four dwarfs of type G5 to K2; the large scatter within a given spectral type is, in fact, largely due to differences in absolute magnitude. Assume that the equivalent width *W* is determined entirely

* *Ap. J.*, **81**, 187, 1935. † *D.A.O.*, **3**, 1, 1924.

by absolute magnitude M and spectral type t and is related to them in the form

$$W(M, t) = \phi(M) \cdot f(t). \qquad (1)$$

Such an expression assumes that the absolute magnitude effect is the same for all spectral types, which will be true within experimental errors for a limited range of types near Ko. We can determine $f(t)$ to a first approximation by drawing a smooth curve through the plots in fig. 1. Multiplication of the measured widths W by $f(\mathrm{Ko})/f(t)$ will then reduce all the measures to type Ko and permit a determination of $\phi(M)$. A second approximation to $f(t)$ was obtained by multiplying the W's by $\phi(+1)/\phi(M)$ and plotting against t. The two determinations of $f(t)$ are shown below ; a third approximation would not have brought improvement since the two determinations of $\phi(M)$ were practically identical.

	t	G6	G7	G8	G9	Ko	K1	K2	K3	K4
$f(\mathrm{Ko})/f(t)$	1st approx.	1·34	1·26	1·16	1·08	1·00	0·92	0·84	0·77	0·72
	2nd approx.	1·23	1·17	1·12	1·06	1·00	0·90	0·77	0·70	0·65

In fig. 2 we plot $W \cdot f(\mathrm{Ko})/f(t)$ as determined by the second approximation

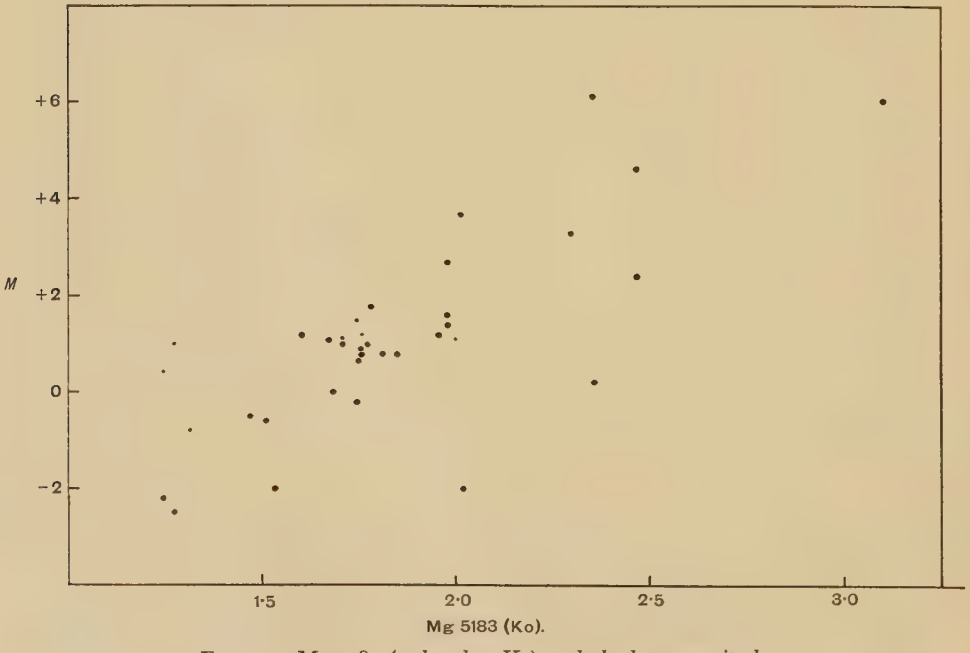

FIG. 2.—*Mg* 5183 (*reduced to Ko*) *and absolute magnitude.*

against absolute visual magnitude (mean of Mount Wilson and Victoria values)*. Owing to increasing uncertainty in $f(t)$ for types considerably

* In one star, ζ Aur, the Mount Wilson absolute magnitude ($-2{\cdot}5$) alone has been used. The Victoria value (0·6 :) is probably affected by the composite nature of the spectrum (cK4 + B), whereas lines in the visual region must correspond to an almost pure K spectrum. It is of interest to note that our measure (outside eclipse) is consistent with the value $M = -2{\cdot}5$.

earlier or later than Ko we have only used stars of type G6·5 to K4. The systematic variation with absolute magnitude is very apparent, and a correlation coefficient of 0·75 has been derived from the data. The intensity increases more than twofold from supergiants ($M = -2$) to dwarfs ($M = +6$). This variation is not entirely independent of temperature, since dwarfs are known to be hotter than giants of the same type, but since *Mg* 5183 is *stronger in dwarfs* the real variation with absolute magnitude at constant temperature is even more rapid than that shown in fig. 2. The data are as yet insufficient to determine whether the absolute magnitude effect changes appreciably along the spectral sequence ; if the observations are divided into two groups earlier and later than Ko, the change is found to be small enough to justify the assumption involved in (1), but, if anything, *Mg* 5183 is slightly *more*

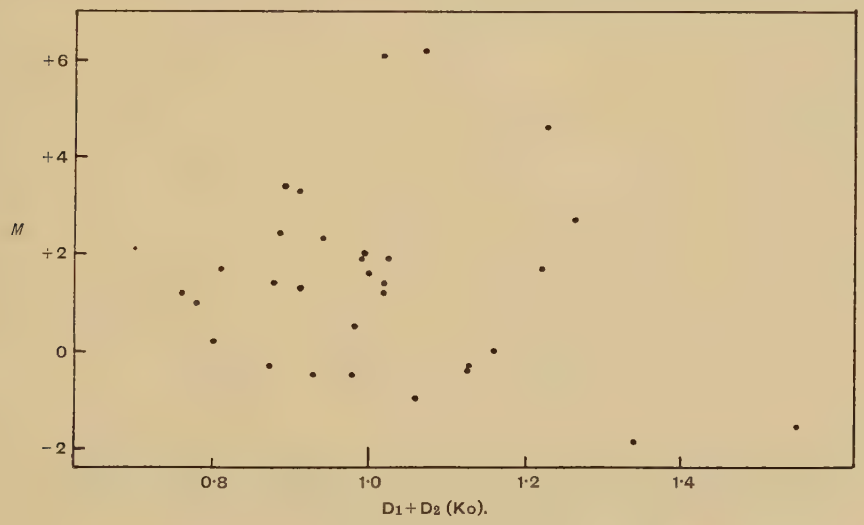

Fig. 3.—*D lines (reduced to Ko) and absolute magnitude.*

sensitive to surface gravity in the later types. The change from giant to dwarf is so marked that this line might well prove useful in detecting dwarf characteristics with very low dispersion even when the "*b*" group is unresolved (*e.g.* in spectra of extra-galactic nebulæ). The residual scatter in fig. 2 may in some cases be ascribed to errors in spectral type which are suggested by intensities of other lines ; a number of marked deviations, however, cannot be explained in this way and these are most naturally attributable to abnormal abundance ; such deviations will be considered in detail in a later paper when more observations are available.

For comparison with this marked absolute magnitude effect of *Mg* 5183 we show similar plots of *Na* 5890, 5896 in fig. 3, and *Fe* 5269, 5328, 5371 (mean) * in fig. 4 against *M*. Intensities have been reduced as before to Ko, a separate determination of $f(t)$ being of course made for each element.

* Owing to blends (chiefly with neutral metals) only central intensities of the *Fe* lines have been measured. With the resolving power used, these should give a good measure of total absorption.

Apart from two supergiants showing strong lines, there is no systematic dependence of these lines on surface gravity. Comparison of the scales of intensity in the two figures shows that there is less dispersion in intensity of *Fe* lines than of the D lines. This is not surprising in view of the fact that spectral type is largely determined by the strength of *Fe* lines. When one takes account of the difference between giant and dwarf temperatures, the

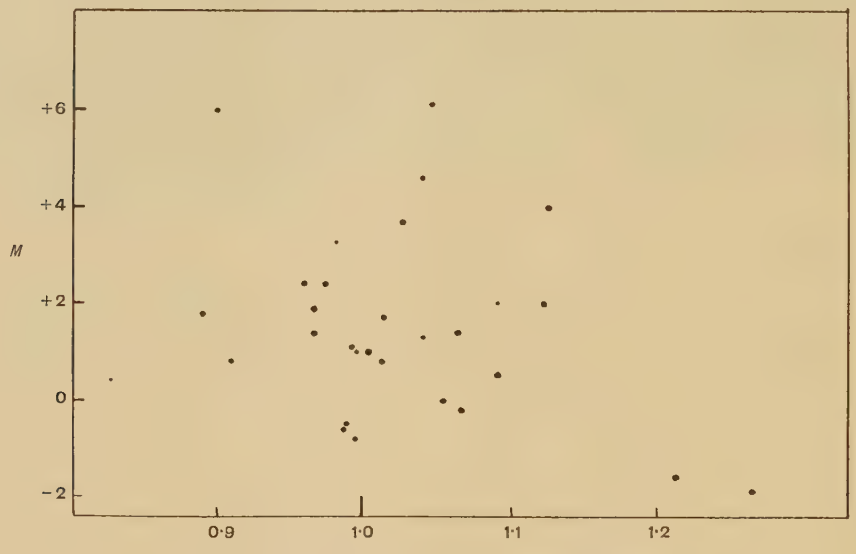

FIG. 4.—*Fe* (*reduced to* K0) *and absolute magnitude.*

null effect for the D lines is seen to be consistent with Unsöld's * calculations that the lines should be somewhat stronger in dwarfs at the same temperature.

In view of the peculiar behaviour of *Mg* 5183 it is highly desirable to examine other lines of *Mg*. The only other available line of sufficient intensity in this region is λ 5528 ($3P^\circ - 4D$, E.P. 4·3 volts) and even this is so weak that only approximate measures of intensity are possible. This line is near its maximum intensity at K0, and consequently no correction factor for type has been applied and the measured intensities are directly plotted against *M* in fig. 5. The uncertainties of the measures preclude definite conclusions concerning this line, but its behaviour appears to differ from that of *Mg* 5183. As before, the line appears to be stronger in dwarfs than in subgiants and normal giants, but in supergiants the line appears strong again. It is very probable, however, that this is due to a neighbouring line, Sc^+ 5526·8, which presumably strengthens in giants. Observations of *Mg* 4703 should decide the point.†

Discussion.—The observed strengthening of *Mg* 5183 in K0 dwarfs is at variance with the behaviour predicted by Russell ‡ and Pannekoek § on

* *Physik der Sternatmosphären*, p. 342.

† The ultra-violet line *Mg* 3838 has been found to be stronger in K type dwarfs by Aller and Stoddard (*Ap. J.*, **87**, 63, 1938).

‡ *Ap. J.*, **78**, 289, 290, 1933. § *Publ. Astr. Inst. Amsterdam*, No. 4, 73, 1935.

the basis of ionization theory according to which the line should show a positive effect at temperatures below 5000°. The failure of the ionization theory to account for the phenomenon is most apparent on comparing figs. 2 and 4. The *Fe* lines used in fig. 4 have E.P. 0·9 volts and I.P. 7·8 volts; for *Mg* 5183 we have E.P. 2·7 volts, I.P. 7·6 volts. Consequently ionization theory would predict practically identical absolute magnitude effects for the lines of the two elements. One might, of course, avoid the difficulty by concluding that *Mg* is more abundant in dwarfs, and this possibility should not be forgotten, although at present it would seem to be an unwarrantable assumption, at least until the behaviour of *Mg* 5528 or 4703 has been established. A more satisfactory explanation would be in terms of some form of line-broadening (additional to natural broadening)

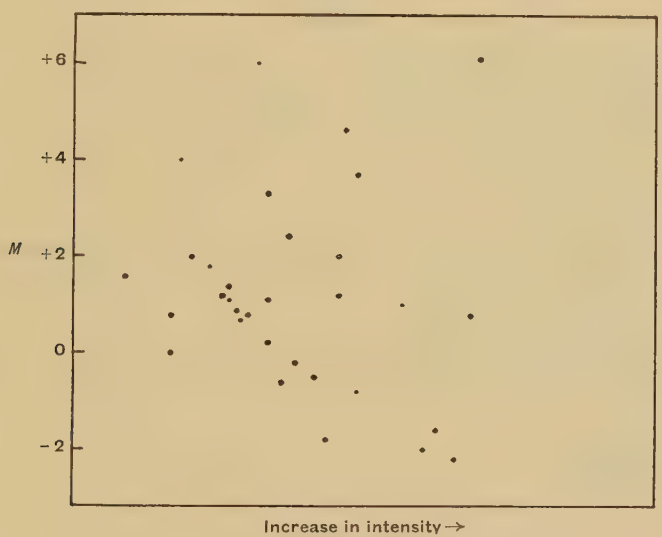

Fig. 5.—*Mg* 5528 *and absolute magnitude.*

which increases with pressure. The behaviour of the diffuse *Mg* series, of which λ 5528 is a member, in the solar spectrum has led Unsöld* to conclude that these lines are largely formed by collisional broadening analogous to Stark effect due to the action of the electric field of passing electrons. Such a broadening would, as Unsöld points out, vary from line to line, and in consequence of the high pressures in dwarfs produce marked negative absolute magnitude effects (such as observed here in *Mg* 5183) in those lines in which it plays a major rôle. It is doubtful, however, whether the variation of *Mg* 5183 can be attributed to this cause in view of the fact that Eckarth† has found this line to show a much smaller shift in electric fields ($-2{\cdot}3$ cm.$^{-1}$ at 690 kV./cm.) than the other *Mg* lines.‡ One further

* *Op. cit.*, p. 273 *et seq.* † *Zs. f. Phys.*, **107**, 182, 1937.

‡ This does not necessarily exclude the possibility of collisional broadening due to a large coefficient ϵ (Eddington notation) for *Mg* 5183. The behaviour of the line at the extreme limb of the Sun (*M.N.*, **97**, 675, 1937) does in fact lend some support to such a hypothesis.

possibility remains to be mentioned. Various *Mg* lines are known to be common features in the emission spectra of M*e* variables; if the lack of balance between emission and absorption is also present (to a less extreme degree) in the atmospheres of K giants it would produce negative absolute magnitude effects unpredicted by ionization theory. None of the explanations offered above for the behaviour of *Mg* 5183 can be regarded as thoroughly satisfactory, and one must wait until further observations of absolute magnitude effects in other lines are available.

It is a pleasure to record thanks to the staff of the Solar Physics Observatory, Cambridge, for their collaboration in the collection of the material used here, which has involved considerable observing time.

Summary

(1) Photometric measures of intensity of *Mg* 5183 in 41 stars of type G5 to K6 show that the line is very sensitive to surface gravity, increasing more than twofold in equivalent width from supergiants to dwarfs of type K0. The *Mg* "*b*" triplet might prove useful in detecting dwarf characteristics on very low dispersion.

(2) The D lines (*Na*) and *Fe* 5269 are insensitive to absolute magnitude (comparing giants and dwarfs of the same type); *Mg* 5528 is probably stronger in dwarfs than giants, while an apparent strengthening in supergiants may be due to a Sc^+ blend.

(3) The behaviour of *Mg* 5183 is at variance with ionization theory. Various possible explanations are considered.

Solar Physics Observatory,
Cambridge:
1939 *April* 4.

SOME HYDRODYNAMICAL EXPERIMENTS IN CONNECTION WITH PROMINENCES

H. Zanstra, Radcliffe Travelling Fellow in Astronomy

(Communicated by the Director, University Observatory, Oxford)

1. *Introduction.*—The streamers which frequently occur in prominences present a rather curious phenomenon. They usually emerge from more extended bright regions above the solar surface in the form of arcs along which bright knots move in predominantly downward directions. Fig. 1,* reproduced with the permission of Dr. Lyot, shows the photograph of a typical prominence of this kind taken by him (1937 June 26 at $8^h\ 59^m{\cdot}5$). The motion of the bright knots along the streamers is best seen in motion pictures of prominences where it is speeded up, so that an actual occurrence taking ten minutes is shown in a time of the order one second. Such pictures taken by means of his coronograph were shown by Dr. Lyot at the Stockholm meeting of the International Astronomical Union in August 1938, and they induced the author to conceive the experiments discussed in the present paper. The first motion pictures of prominences were taken by McMath in monochromatic light. In the November meeting of the Royal Astronomical Society, 1938, Dr. Curtis has shown more recent films from the McMath-Hulbert Observatory which also show the movement along the streamers very clearly.

Naturally, a perfectly stationary stream would not give any impression of motion in a moving picture film. The phenomenon is rather that of bright lumps and knots moving along rather definite curved tracks, and this can hardly be interpreted otherwise than that luminous matter is actually moving along such tracks. The alternative explanation that there is an exciting agency which moves along in a stationary gas would encounter great difficulties, since it is hard to conceive of an agency like ultraviolet radiation or electrons or ions which moves along in the form of lumps. This naturally raises the question whether there are not some terrestrial experiments in which a stream of matter is confined to rather definite tracks and which could provide some analogue to the streamers in prominences.

Such an analogue seems to be provided by the experiments to be discussed in the next section. The phenomenon is briefly this. If water, under a pressure of the order 1 cm., is made to enter through a hole of diameter, say, 2 mm. in the bottom of a basin, the water does not spread out into the basin evenly in all directions, but goes outward in the form of a few rather thin currents or streamers separated by quieter regions. We shall refer to this phenomenon as the "streamer phenomenon". Fig. 3 shows

* Figs. 1 to 16 are all photographs reproduced in Plates 7 and 8. The two diagrams in the text are indicated by Roman figures : figs. I, Ia and II.

the experiment for water in a basin photographed from above. The outward currents or streamers are made visible by talcum powder. There are two such streamers, one going off to the right (*a*) and one shorter one to the left (*b*). Outside these streamers the liquid moves more quietly in the form of whirls, resulting in two broader inward streams very roughly perpendicular to *a* and *b*. Visually the outward streamers are more conspicuous than on a photograph, because one sees them moving with a much larger velocity than the rest. On a photograph the streamer phenomenon is perhaps shown more convincingly in fig. 4, where the liquid emerging from the hole has been coloured with iodine and starch. There one clearly sees two outward streamers *a* and *b*, and, less clearly, a third one *c*.

The experiments appear to be of direct hydrodynamical interest, and we shall first discuss them for their own sake. So section 2 will be taken up by a discussion of experiments of flow of liquid entering by a hole in the bottom of a basin, where streamers are produced in certain cases and a purely radial flow of liquid in other cases. This will be followed, in section 3, by a discussion of the condition for instability which determines the occurrence of the streamers and its application to an ideal liquid. Section 4 is taken up by the theory for a viscous liquid. A point of doubt raised by the experiments in an open basin is settled in section 5 in favour of the theory by the experiments under glass, which eliminates the surface tension.

The discussion of the experiments and theory take up the larger part of the paper. There seems to be ample justification for this, since both the phenomenon and its explanation have not been treated before, and to make the treatment convincing requires a thorough discussion. After the necessary theoretical background has thus been developed, astrophysical applications, though eventually supported by experimental models, do not have to depend on mere analogies.

Reserving a more thorough discussion for a future paper, the general application to prominences will be shortly dealt with in the last section. In this section it is made plausible that streamers originate in virtue of the same condition for instability which applies to the liquid experiments, and this is further supported by an experimental model. It is further suggested that streamers are made luminous in a non-luminous medium by a mechanical excitation, but this is not proposed as the source of luminosity of prominences in all stages of development.

2. *Experiments with Open Basin for Various Liquids. Flows of Current Type and Radial Type.*—Fig. 2 is a photograph of the apparatus used in the experiments. The liquid is poured into the basin P on the right, which will be termed the pressure basin, since the applied pressure is varied by either varying the height of the liquid in the basin, read on a scale *s* on its rim, or by moving it up and down on the stand S which carries it. A rubber tube T of a diameter of 1 cm. and variable length connects the pressure basin P with a cylindrical reservoir. From the cylindrical reservoir the liquid flows out into another basin E through a hole of a diameter of 1·7 mm. in its bottom, while it leaves in front by an outflow hole of diameter 5 mm., under which is placed the receptacle R. In some experiments the outflow

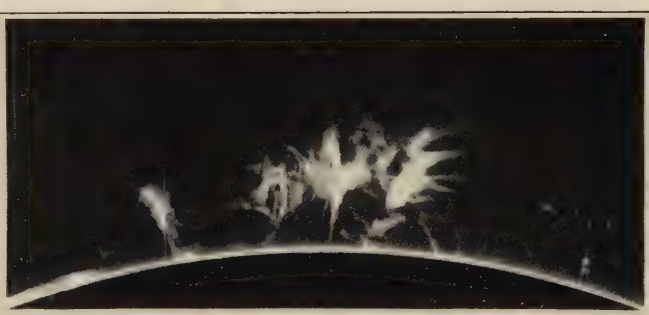

FIG. 1.
Prominenc Streamer (Lyot).

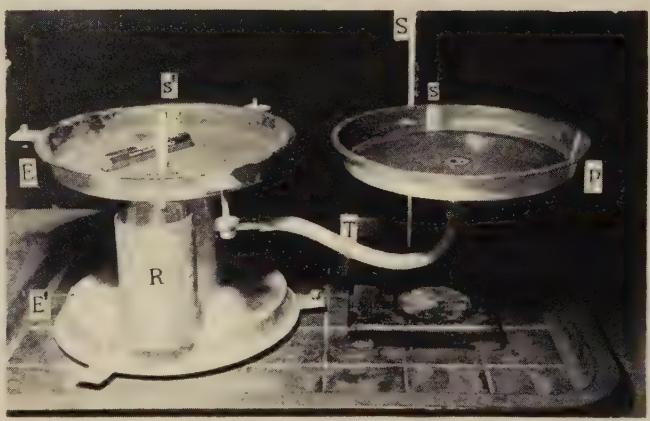

FIG. 2.
Apparatus

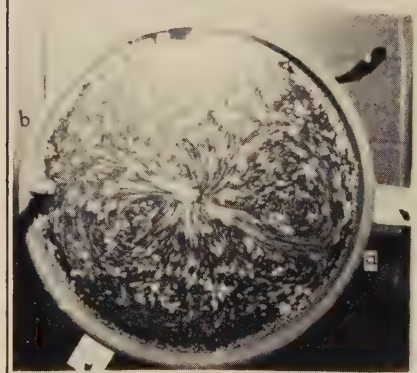

FIG. 3.
Water. Streamers on surface.

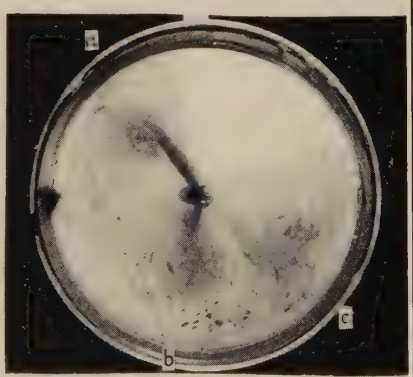

FIG. 4.
Water. Streamers also below surface.

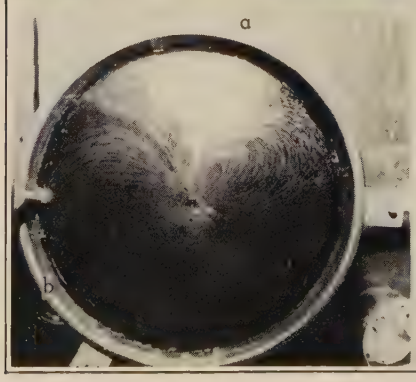

FIG. 5.
Water. Streamers.

FIG. 6.
Glycerine 43 per cent. Streamers.

H. Zanstra, Some Hydrodynamical Experiments in Connection with Prominences.

FIG. 7. *Glycerine 43 per cent. Radial flow.*

FIG. 8. *Glycerine 81 per cent. Radial flow.*

FIG. 9. *Water. Inward flow.*

FIG. 10. *Alcohol open*

FIG. 11. *Alcohol covered.*

FIG. 12. *Water covered.*

FIG. 13. *Glycerine 81 per cent. covered.*

FIG. 15. *Slit 4 cm.*

FIG. 14. *Slit 17·3 cm.*

FIG. 16. *Slit 2 cm.*

is entirely open, but mostly it is partly closed by a wooden plug p, which increases the height of the liquid, read on the scale s', to any value desired. It is in this experiment-basin E that the phenomenon of liquid-flow to be observed takes place. The foot of the apparatus consists of a similar basin E′ upside down to which three levelling screws are attached. It has a hole of 3·3 mm. in the centre which is plugged up when the apparatus is used with E as experiment-basin. The internal diameter of the bottom of the three basins P, E and E′ is 18·8 cm. The basins are adjusted horizontally by means of a spirit-level also seen in fig. 1.

To use the basin E′ with the hole of 3·3 mm.—in which, by the way, the outflow is on the left—one puts the apparatus upside down and adjusts it by the three levelling screws attached to E. Because liquid may be spilled, the apparatus is placed on a tray. When the experiment is actually in progress the liquid which collects in the receptacle R is poured back into P at short intervals to maintain an approximately constant applied pressure $p_0 = s - s'$ (the difference of the two scale readings). If the two basins are not on the same level, this pressure should be increased by the upward displacement of P along S.

The outflow in cm.^{3} per second, which is termed Q for an open basin, is determined by collecting and measuring the outflowing liquid for a short interval timed by a stop-watch.

To make the currents or the flow on the surface of the liquid in E visible, talcum powder or metal powder (bronze as used for artificial gold paint or aluminium as used for aluminium paint) is shaken on to the surface.

The photographic arrangement consists of a Voigtlander Brillant V6 camera with portrait lens. It is mounted vertically above the centre of the experiment basin at a distance of 61 cm. The basin was illuminated by an Osram Photoflood lamp of 250 volts. The time of exposure generally was about 1·5 second.

When a photograph was taken or a visual observation carried out, a number of quantities determining the conditions of the experiment was measured ; in the case of photographs this generally was done immediately after the exposure.

Table I contains the results of the observations in an open basin E or E′ as just described. The first column gives the liquid investigated, followed by the density ρ, the viscosity μ and the surface tension σ, all in C.G.S. units for a temperature of 18° C., which was roughly that of the experiments.*

* The values for water, mercury, turpentine and ethyl alcohol were obtained by interpolation between 10° and 20° from Kaye and Laby, *Physical and Chemical Constants*, Longmans Green, 1936 ; for glycerine and glycerine-water mixtures from Landolt-Björnstein, *Physikalisch-Chemische Tabellen*, I, pp. 458, 136; the surface tension of glycerine, 43 per cent., was measured by the height in a capillary tube compared with that of water. The density of the glycerine, 81 per cent. and 43 per cent., was checked, and, roughly, also the μ and σ of the liquids used, excepting the σ for 100 per cent. glycerine. The alcohol actually used was commercial methylated spirit, which consists chiefly of ethyl alcohol (90 per cent.) and methyl alcohol (9 per cent.), but since the experiments are not accurate, the constants for ethyl alcohol were used instead.

The second column indicates by the letters p or v whether the experiment was photographic or visual, the number in parentheses is the number of photographs or independent visual observations. Columns 3, 4 and 5 give the conditions which permit the reproduction of the experiment but are not of direct theoretical interest, namely, the diameter (cm.) of the inflow hole in the bottom of the experiment basin, the length of the rubber tube T in cm.,

TABLE I

Observed Flows of Streamer Type or Radial Type. Open Apparatus

(For a flow of the streamer type the average length in cm. r_s of the currents is given in the last column. A flow of radial type is marked by R.)

1 Substance and Physical Constants	2 Phot. or Vis.	3 Diam. Hole cm.	4 Tube T cm.	5 p_0 cm.	6 Q cm.^{3}/sec.	7 h cm.	8 Calc. r_{cr} cm.	9 Obs. r_s or R	Remarks
Water:	$p(10)$	0·17	22	0·1	0·30	1·6	2·4	6·7	Fig. 3
$\rho = 0{\cdot}998$	$p(2)$	0·17	22	1·0	1·04	0·4	2·2	4·5	(1) Fig. 4
$\mu = 0{\cdot}0107$	$p(2)$	0·17	22	1·1	1·13	0·15	1·4	4·2	Fig. 5
$\sigma = 73$	$p(1)$	0·33	22	0·25	1·45	0·08	1·2	4·0	
	$v(2)$	0·17	40	1·4	0·48	0·15	0·9	1·9	(2)
Glycerine 43 per cent.:	$p(1)$	0·33	22	1·0	2·5	0·35	1·7	2·7	Fig. 6
$\rho = 1{\cdot}108$	$v(1)$	0·33	153	1·6	2·2	$\sim 0{\cdot}15$	$\sim 1{\cdot}0$	S	
$\mu = 0{\cdot}0432$	$p(1)$	0·33	22	0·6	1·80	0·15	0·9	R	Fig. 7
$\sigma = 59$	$v(1)$	0·33	153	1·0	1·67	$\sim 0{\cdot}15$	$\sim 0{\cdot}9$	R	
Glycerine 81 per cent.:	$v(1)$	0·33	153	21·4	4·5	0·8	0·9	R	(3)
$\rho = 1{\cdot}215$	$p(2)$	0·33	40	3·5	2·5	0·5	0·5	R	Fig. 8
$\mu = 0{\cdot}732$									
Glycerine 100 per cent.:	$v(1)$	0·33	153	50	0·44	0·5	0·06	R	
$\rho = 1{\cdot}263$									
$\mu = 10{\cdot}69$									
$\sigma = 65$									
Alcohol (4):	$p(3)$	0·33	22	0·4	1·18	0·3	1·7	R	(4) Fig. 10
$\rho = 0{\cdot}79$									
$\mu = 0{\cdot}0125$									
$\sigma = 22$									
Turpentine:	$v(1)$	0·17	40	0·4	0·50	0·25	1·0	R	(5)
$\rho = 0{\cdot}865$									
$\mu = 0{\cdot}0149$									
$\sigma = 27$									

(1) Streamers made visible by iodine-starch.

(2) Inflow by tube 1·1 cm. long, diam. 0·17 cm. Simplified apparatus.

(3) At $p_0 = 66{\cdot}5$ cm. the flow was still Type R, but there was a fountain 1 cm. high which disturbs the conditions.

(4) The physical constants are those for pure alcohol. Actually methylated spirit was used.

(5) Simplified apparatus. Various applied pressures p_0 up to 1·45 cm. were tried, but none of them gave the streamer type of flow. From 0·6 cm. onwards the hill of liquid at the centre became wobbly, and at 1·45 cm. it nearly amounted to a fountain.

and the applied pressure p_0 in centimetres of liquid, being the difference in level of the liquid in P and E. This is followed, in columns 6 and 7, by the quantity of liquid Q flowing out per unit time in cm.^{3}/sec., and h, the height of the liquid in the experiment basin in centimetres, which are both direct determining factors of interest for the theory (section 4). This height h was measured away from the edge by putting a piece of millimetre paper in the liquid; it is not very accurate and, if smaller than 2 mm., hardly better than an estimate. At the edge one gets the influence of capillarity which also makes determination of h in the basin itself hard, since the liquid creeps up against the millimetre paper. Column 8 will be discussed in section 4. Column 9 contains an R if the observed flow of liquid is a radial one going off in all directions, which may occur for other liquids than water. If, however, we have the interesting case of streamers, the average length r_s of the streamers measured is given in centimetres. This is measured from the centre to the point where the stream lines diverge appreciably, and so is, naturally, a somewhat arbitrary quantity. For example, in the rather clear-cut case of fig. 3 the length of 8 cm. was measured for streamer a, and 3·5 cm. for streamer b, and this can readily be verified from the figure, remembering that the diameter of the basin is 18·8 cm. When one of the photographs used for Table I is reproduced in one of the figures of the present paper, this figure is indicated under the Remarks, under which heading also some further particulars are given in the form of footnotes to the table.

The first experiments were done with *water*. The smallest pressure used must have been of the order 1 mm. of water, going up to 1·6 cm. with the 1·7 mm. inflow hole and up to 0·6 cm. with the 3·3 mm. hole. Throughout this range of pressure a clear-cut case of streamers has always been observed for water. It may be described as follows. The water emerging from the hole wants to go upward first, and this gives rise to a little knob or hill of liquid in the centre above the hole.* It then spreads out horizontally across the surface, but does so not as a stream radially outwards in all directions, but in the form of a number of rather thin streamers. One way of making them visible is by colouring the water in the pressure basin P and then waiting until, after having passed through the reservoir, the coloured water emerges from the central hole in the experiment basin E. Fig. 4 shows the experiment basin in this state, photographed from above. The basin was painted white for this experiment †, and the water coloured with

* At too high pressures the centre gets wobbly, and finally a little fountain is formed in the centre.

† The apparatus used was a copy of that just described, with basins painted white instead of black. Some starch (a paste of powdered starch made into a suspension by boiling water) had been mixed with the water, and a few drops of tincture of iodine in the pressure basin produced an intensive blue colour. Due to initial disturbances it takes a little while before the currents get steady enough. So some plumbago powder, which shows up well against the white basin, was shaken on to the surface, and not until the surface currents were steady was the iodine added. (The whirls seen in the picture are due to streaks of this plumbago.)

One may also use ordinary water and add a solution of potassium permanganate to the pressure basin, giving an intense violet colour.

iodine-starch is seen to emerge in the form of two streamers *a* and *b* of lengths 6 and 4 cm. (There is probably a third one in the direction *c*.) From this experiment it follows that the streamer phenomenon is not confined to the surface. Mostly, however, the streamers were studied on the surface only by shaking powder on to it. One may shake a little powder on to the centre, and it is then carried away along the streamers in something like a second, and the streamers become clear again. Powder, however, shaken on the surface outside the streamers is not carried away but circulates almost indefinitely in the form of whirls; *e.g.* in fig. 3 streamer *a* goes to the right, above it the talcum powder shows a left-hand whirl, below it a right-hand whirl. Similarly, *b* going off to the left has a right-hand whirl above it and a left-hand whirl below it. So the typical two-streamer case of fig. 3 consists of two outward streamers each of which is flanked by two whirls. One may also look upon the adjoining portions of the two whirls going outward as an outward streamer, but then it should not be forgotten that the actual streamer emerging from the hole is clear of talcum powder (this clear portion is so thin that it hardly can be seen on the photograph, where it may be entirely obliterated by slight irregularities occurring during the exposure of 1·5 second). Similarly, the inward-going adjoining portions of two whirls may be looked upon as an inward stream. We shall often use the words outward streamer and inward stream in this sense, but wish once more to point out that in doing so we are dealing with circulation currents, whereas each true outward streamer forms a core to an outward circulation current—it emerges from the hole and does not come back, and actually is extremely thin and clear of powder. Very fine metal powder shaken through a small piece of thin cloth on to the surface is most suitable to show all the details which we did not succeed in photographing. Visually the outward streamer is a clear core along which particles of the adjoining whirls are rather suddenly caught and then move so fast that they often appear as thin streaks of, say, 1 cm. long which cannot be followed with the eye—the velocity then must be something like 10 cm./sec.

What determines the number of streamers is hard to say, often there are two outward streamers, often three, in some cases four or more. Sometimes a type of motion changes during the experiment, but often it persists for a quarter of an hour or more; *e.g.* in the first entry of Table I (10 subsequent pictures of which fig. 3 is an example) the two-streamer type persisted for half an hour, but the length of the streamers changed somewhat.

The direction of the streamers seems to have little to do with the place of the outflow hole. Irregularities in the hole, though it is conceivable that they might decide the position of the streamers, probably make little difference for the production of the phenomenon: we got a two-streamer type with a square hole of 1·2 mm., and mostly a two-streamer type with a hole in the form of a slit, 4 mm. long and about 1 mm. wide, with the streamers not quite perpendicular to the slit but inclined over about 30°. Nor does it seem necessary that the liquid enters the hole from below freely in all directions. We made a simplified apparatus in which a brass tube of 1 cm. diameter was directly attached to the experiment-basin and connected with the rubber

tube T, thus dispensing altogether with the reservoir. In another case we made the water from T enter the experiment basin through a tube of length 1·1 cm. and width 1·7 mm., the same as the hole in its bottom. In both cases the streamers were clearly seen with water. For the streamers to occur, the theory to be discussed later only requires that the outflow into the basin soon gets horizontal, and it appears that this condition is sufficiently fulfilled with these other experimental arrangements.

If the experiment lasts long, the surface gets paralysed, and instead of clear outward streamers one may get short loops forming a rosette-like pattern. This may partly be due to the forming of larger aggregates from the powder and partly to dust particles, which can be seen to disturb the thin currents. One can then clear the surface by drawing a sheet of paper across it on which the particles and dust collect, and new powder gives again an undisturbed pattern.

The two-streamer case of fig. 3 occurred for a small applied pressure ~1 mm. and a rather large depth of water $h = 1{\cdot}6$ cm. (see Table I). A much less simple case is presented in fig. 5, $p_0 = 1{\cdot}1$ cm., $h = 0{\cdot}15$ cm. When taking the picture there were a rather large number of streamers, but one can only clearly see one streamer *a* of length 3 cm. between two adjacent whirls and another one *b*, less clear, of length 5·5 cm., so the r_s adopted for this picture was 4·2 cm. Altogether the case is often more complicated than fig. 3, where each outward streamer was flanked by two whirls; it often is so that only one of the adjacent whirls for a streamer is clearly pronounced.

The question now arises whether the streamer phenomenon is determined by the absence or presence of viscosity or whether there are some more determining factors.

When the phenomenon is purely determined by viscosity, Reynolds' * fundamental considerations show that, if *a* is a characteristic distance, *e.g.* the average distance, and *w* a characteristic velocity, *e.g.* the average velocity, then, for similar apparatus, the quantity

$$N_R = \frac{\rho}{\mu} wa \qquad (1)$$

determines the stream lines (*Reynolds' Law of Similarity*), and that in general large N_R favours turbulent flow. So the more viscous the liquid, or, more precisely, the larger μ/ρ, the harder it is to get the N_R corresponding to a certain amount of turbulence, because the required velocity *w* gets larger.

In other words, one may expect large μ/ρ to favour laminar flow, viz. in our case radial flow, and small μ/ρ to favour non-laminar or turbulent flow, viz. our streamer case. This indeed is shown to be the case by the *experiments with glycerine and mixtures of glycerine and water* (see also Table I). Passing from water, $\mu/\rho = 0{\cdot}0107$, to glycerine 43 per cent., $\mu/\rho = 0{\cdot}0400$, we get a streamer case in fig. 6, but a case of radial flow in fig. 7, where the applied pressure was smaller. Fig. 7 was obtained by shaking bronze powder all

* Reynolds, *Phil. Trans. Roy. Soc. London*, **174**, 935, 1884. A simple derivation is given in Prandtl-Tietjens, *Applied Hydrodynamics*, p. 8, McGraw-Hill, 1934.

over the surface, and it is seen to flow outwards. The radial flow is not evenly in all directions, but shows yet a bias for currents, yet this radial type of motion, marked *R* in Table I, is altogether different from the streamer case, since the bronze powder wherever deposited moves outward and does not circulate in whirls as in fig. 6.

The still higher value of $\mu/\rho = 0{\cdot}60$ for glycerine 81 per cent., as may be expected, is a still clearer case of radial flow shown in fig. 8. Here some bronze powder on a knife-point was deposited several times in succession at the centre, and it is seen to move outwards in concentric rings which come close together on one side (rather oddly, this happens to be the side at which the outflow occurs). In the visual experiments this type of outflow persisted to an applied pressure of 66 cm.

Experiments with pure glycerine, $\mu/\rho = 8{\cdot}5$, all done visually, gave a case of radial flow for all applied pressures up to 132 cm.

The foregoing considerations based on Reynolds' Law only serve as an orientation, making it likely that low viscosity per unit mass is the main factor favouring the phenomenon of streamers. A more detailed theory is discussed in the next two sections. The experiments with alcohol and turpentine, both of small surface tension, will be discussed after the theory is given, at the end of section 4.

3. *Ideal Liquid. Conditions for Stability and Instability. Unstable Outward Motion.*—In proposing a theoretical explanation of the current phenomenon, we shall first consider *an ideal liquid streaming in between two equidistant plates.* Let the separation of the plates be $2h$, and assume that the liquid, by some mechanism, is made to move radially outward from a certain axis such that the velocity v is parallel to the plates and independent of the depth, that there is radial symmetry about this axis, and that the motion is stationary. Let the radius, or distance from the axis, be denoted by r, and for the range of r studied let there be no other force than that due to pressure.

The volume of the liquid moving outward per second may be denoted by $2Q$, which is independent of the time, since the motion is stationary. For one half of the apparatus the height is h and the outflow Q, and our considerations in this as well as in the case of section 4, where the viscosity is considered, are to be given *for the one half*, the two halves being symmetrical with respect to the plane of symmetry half-way between the plates.

The equation of continuity is $Q = 2\pi rhv$ or

$$v = \frac{Q}{2\pi rh} = \frac{k}{r}, \tag{2}$$

so that the velocity decreases outwardly.

The relation between the pressure p and the velocity is given by Bernouilli's Law,

$$p + \tfrac{1}{2}\rho v^2 = \text{const.}, \qquad \frac{d}{dr}(p + \tfrac{1}{2}\rho v^2) = 0, \tag{3}$$

where the density ρ is a constant for an ideal liquid.

From (2) and (3) follows $$\frac{dp}{dr}=\frac{\rho k^2}{r^3}. \tag{4}$$

In order to see whether the above radial solution is stable, we create the following disturbance. Using polar co-ordinates r, θ, we change, at a certain instant $t=0$, the velocities in a small sector $\Delta\theta$, by changing the k by δk for each $d\theta$ within $\Delta\theta$, the δk being zero at the two boundaries of $\Delta\theta$, so that no discontinuities occur. The disturbed velocity is therefore, at this instant, given by

$$v=\frac{k+\delta k}{r} \tag{5}$$

and directed radially.

The hydrodynamical equation of motion in Cartesian co-ordinates x, y is, for the x direction,

$$-\frac{1}{\rho}\frac{\partial p}{\partial x}=\frac{\partial v_x}{\partial t}+v_x\frac{\partial v_x}{\partial x}+v_y\frac{\partial v_x}{\partial y}. \tag{6}$$

Taking r along the axis of x, we have $v_x=v$ and $v_y=0$, for the disturbed motion at the instant considered, so that

$$\frac{\partial v}{\partial t}=-\frac{1}{\rho}\frac{\partial p}{\partial r}-v\frac{\partial v}{\partial r}. \tag{7}$$

Since, except for the infinitesimal region $\Delta\theta$, the motion is undisturbed, the pressure should not only approach its normal value (4) for regions a little outside $\Delta\theta$, but also one may expect this normal value to be impressed on the very narrow disturbed sector.* Substituting the value (4) for the pressure and (5) for the velocity, the expression (7) reduces to

$$\frac{\partial v}{\partial t}=2\frac{k\delta k}{r^3}=2\frac{k}{r^2}\delta v, \tag{8}$$

where the disturbance in velocity $\delta v=\delta k/r$, being the difference of (5) and (2), has been introduced. Equation (8) gives us the local change in velocity for the disturbed motion at $t=0$ or immediately following.

The *conditions for stability and instability* of radial motion may now be expressed as follows. If, subsequent to a disturbance, $\frac{\partial v}{\partial t}$ has a sign opposite to that of the velocity disturbance δv, the motion will return to its undisturbed state and is therefore stable for the type of disturbance considered. If, on the other hand, $\frac{\partial v}{\partial t}$ has the same sign as δv, the liquid will become further removed from the undisturbed state, and this state certainly is unstable.†

We shall first consider an outward radial motion, since this is the case

* This assumption, "undisturbed pressure for the disturbed motion", requires further justification. A rigorous treatment of instability, based entirely on the laws of hydrodynamics, is desirable.

† Since instability cannot always be judged by the *initial* deviation, the considerations given here and in section 4 may require modification. Their present use is that they give an orientation of a rather large number of facts.

of our experiments. Outward radial motion from the centre means that v, and hence k in (2), is positive. Then (8) $\frac{\partial v}{\partial t}$ has the same sign as δv and satisfies the condition for instability. *For outward radial motion the radial solution of radial symmetry is therefore unstable.*

Stated in non-mathematical language, the previous proof amounts to the following. For the motion considered, the velocity is outward and indirectly proportional to r, the acceleration inward and indirectly proportional to r^3. If then, in a small sector, all velocities are increased in the same ratio, the new motion can only be kept going by a larger inward acceleration within this sector. The existing pressure force giving the old inward acceleration is therefore unable to keep the new motion in check, and the disturbance increases still further. (For liquid diverging radially from a point in all directions in space, the velocity is outward and indirectly proportional to r^2, the acceleration inward and indirectly proportional to r^5, and the motion is unstable for the same reason.)

All this, then, seems to be the gist of the explanation of the streamer phenomenon, which is favoured by small viscosity and so certainly should occur for an ideal liquid. The radial solution for outward motion is unstable ; we have in our basin certain regions where the liquid goes outward much quicker than the average, namely the streamers, and other regions where it goes more slowly, even going inward at the inward streams.

The above case of motion between two plates is really that of a covered basin, actual examples of which will be given in section 5. An ideal liquid in an open basin is represented by the lower half of the solution. The influence of gravity would then result in the h decreasing a little outwardly, but if the outflow is slow enough this does not amount to much and its approximate constancy for equation (2) is ensured. The pressure p is then really the pressure along the bottom of the basin. The rôle of the pressure difference between two points 1 and 2 in the undisturbed motion is merely that of the work gained per volume-element for liquid transported. On the surface of the liquid under gravity this is $\rho g(h_1 - h_2) = p_1 - p_2$ in terms of the pressure at the bottom, and the same thing holds if the points are on a stream line intermediate between surface and bottom. Since we have been dealing with the undisturbed pressure throughout, all formulæ can be retained for an open basin, even if there is gravity.

An example of stable radial flow is a converging stream, obtained by reversing the motion in the above example. For such a stream k in (2) is negative, and then it follows from (8) that $\frac{\partial v}{\partial t}$ has a sign opposite to that of δv, which is the condition for stability. Such a converging stream is therefore stable for radial disturbances, even for an ideal liquid. Experimentally it was realised for water flowing out of a basin through a central hole. A photograph of this stream is seen in fig. 9, and the perfect symmetrical flow is in marked contrast to the streamer flow of figs. 3 to 5.

4. *Viscous Liquid. Radial Stream between two Parallel Plates, or along one Plate. Approximate Theory for the Length of the Currents. Comparison*

with Observation.—In this section we shall consider the same problem as in section 3, but now for a viscous and incompressible liquid. The motion between the plates is stationary and, when undisturbed, is radially outward, and has radial symmetry about an axis perpendicular to the plates. Again, the distance of each plate to the plane of symmetry is h, and the co-ordinates of any point are now the distance r from the axis, the perpendicular distance z from the plane of symmetry and the angle θ which the projection of r on the plane of symmetry makes with a certain fixed direction. As in section 3, we consider everywhere only one half of the apparatus.

Unlike the case of an ideal liquid, the velocity at any point r, θ must now vary with z. *For large* r the stream becomes parallel, then there is no acceleration, and the pressure force makes equilibrium with the viscosity force, which is therefore independent of the depth. From this easily follows that for large r

$$v = V\left(1 - \frac{z^2}{h^2}\right), \tag{9}$$

if V is the velocity in the plane of symmetry $z = 0$. This distribution is represented by the parabola in fig. Ia, at the bottom of fig. I. From (9)

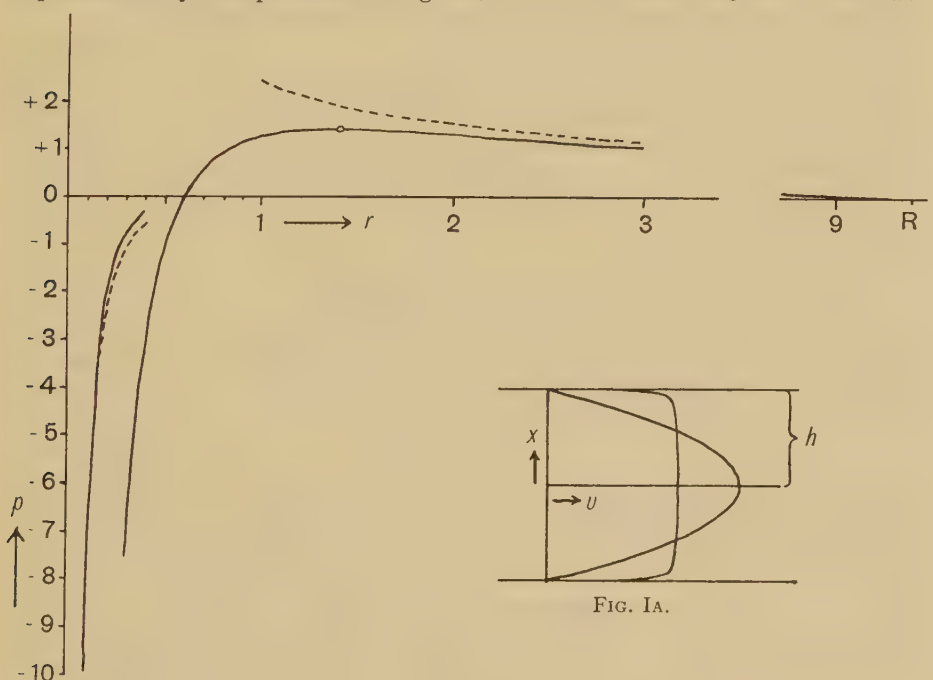

Fig. Ia.

Fig. I.

Fig. I.—*Radial solution* $p = ln\frac{R}{r} - \left(\frac{1}{r^2} - \frac{1}{R^2}\right)$. *For lower values of* r *the curve is continued on a ten times smaller scale. The dotted line at large r refers to the logarithmic term, and at small r to the inverse square term. The part for r smaller than* $r_{cr} = 2$ *is unstable, and the maximum pressure occurs at* $r_M = \sqrt{2}$.

Fig. Ia.—*Assumed parabolic distribution of velocities. For small r the actual distribution should approach a rectangular one, as is schematically indicated.*

follows the average velocity and average (velocity)^2:—

$$\bar{v} = \frac{1}{h}\int_{z=0}^{h} v\,dz = \tfrac{2}{3}V, \tag{9a}$$

$$\overline{v^2} = \frac{1}{h}\int_{z=0}^{h} v^2\,dz = \tfrac{8}{15}V^2. \tag{9b}$$

As we approach the centre, the mass-acceleration force becomes of more importance, and we finally expect to get to a stage where this force makes equilibrium with the pressure force. This can be done by a stream of velocity independent of the depth and parallel to the plates as considered in section 3, and so, *for small r*, we are approaching the case of an *ideal liquid* discussed there. Only at the very edges the velocity has to come down to zero, and the viscosity force may become important, and so we shall get the situation schematically represented by the other profile in fig. Ia, which is nearly rectangular.

The immediate consequence of this is that the stream lines for intermediate r cannot be parallel to the plates, but that going outwards they should converge near the plane of symmetry and diverge near the plates.

Being aware of this fact, we shall nevertheless only *give a solution for a parabolic velocity distribution* (9) and resulting stream lines parallel to the plates (but directed radially). At infinity this will give us the correct solution, and for finite distances we shall be content with estimating the error, being satisfied if we are not off by a too large factor.

Since under this approximation all stream lines are straight, the *condition of continuity* results in

$$V = \frac{k}{r}, \qquad v = \frac{k}{r}\left(1 - \frac{z^2}{h^2}\right), \tag{10}$$

the latter equation following from (9). The total outflow per unit time is $Q = 2\pi r h \bar{v}$, to which k is related by

$$k = \frac{3Q}{4\pi h}, \tag{11}$$

as follows from (9a) and (10).

The *equation of motion* reduces for radial stationary motion to

$$f_\mu - \frac{1}{\rho}\frac{\partial p}{\partial r} = v\frac{\partial v}{\partial r} = \frac{\partial}{\partial r}(\tfrac{1}{2}v^2), \tag{12}$$

where f_μ is the viscosity force per unit volume and ρ the constant density. For the case considered this force is directed along r and given by

$$f_\mu = -\mu\frac{\partial^2 v}{\partial z^2} = -\frac{2\mu k}{h^2 r}, \tag{13}$$

as follows from (10).

With the assumed velocity distribution (9) it is not possible, except at infinity, to satisfy the equation of motion (12) rigorously. If satisfied for one value of z, deviations occur for other values of z. The most suitable

approximation seems to be that the equation (12) is satisfied on the average as regards z. So we adopt the equation of motion

$$f_\mu - \frac{1}{\rho}\frac{\partial p}{\partial r} = \frac{\partial}{\partial r}(\tfrac{1}{2}\bar{v}^2), \tag{14}$$

where we still may use (13) for f_μ, being independent of z. Another way of stating this approximation is that for a vertical column of liquid extending between the two plates the total force is in equilibrium with the total mass acceleration, and thus the mechanical law satisfied for such a column.

Substituting (13) in (14) and using (9*b*) and (10), we obtain the *differential equation for the pressure*

$$\frac{dp}{dr} = -2\frac{\mu k}{h^2 r} + \frac{8}{15}\frac{\rho k^2}{r^3}. \tag{15}$$

Introducing Q by (11), this equation may also be written

$$\frac{dp}{dr} = -\frac{3}{2}\frac{A}{r} + \frac{3}{10}\frac{B}{r^3}, \tag{16}$$

where

$$A = \mu\frac{Q}{\pi h^3}, \tag{16a}$$

$$B = \rho\left(\frac{Q}{\pi h}\right)^2. \tag{16b}$$

From (16) it follows that the pressure has a maximum value p_M at $r = r_M$ given by

$$r_M = \sqrt{\frac{1}{5}\frac{B}{A}} = 0{\cdot}447\sqrt{\frac{\rho}{\mu}\frac{Qh}{\pi}}, \tag{17}$$

where we have put in the numerical value 0·447 of $\sqrt{\frac{1}{5}}$.

For $r >> r_M$ the first term on the right-hand side of (15) or (16) becomes predominant, $\frac{dp}{dr} = -2\frac{\mu k}{h^2 r}$ so that (10) may be written $v = -\frac{1}{2}\frac{h^2}{\mu}\frac{dp}{dr}\left(1 - \frac{z^2}{h^2}\right)$, which is the well-known velocity distribution for a parallel stream between two plates. So for large r our expression is quite correct, as might have been anticipated.

For $r << r_M$ the second term on the right-hand side of (15) or (16) becomes predominant, so that $\frac{dp}{dr} = \frac{3}{10}\frac{B}{r^3} = \frac{3}{10}\rho\left(\frac{Q}{\pi h}\right)^2 \Big/ r^3$, whereas we should approach the case of an ideal liquid of section 3, where (4) and (2) lead to $\frac{dp}{dr} = \frac{1}{4}\rho\left(\frac{Q}{\pi h}\right)^2 \Big/ r^3$. So for small r the result of equation (16) is too high by a factor 1·2. So it seems that the accuracy is about 20 per cent.*

* From the two limiting cases it may be seen in a very elementary way that the pressure should show a maximum as follows. Near the source the retardation approaches infinity, merely on account of the radial spread of the liquid coming out. So there must be a pressure gradient positive outward to produce this retardation. At large r the motion is nearly parallel, and for this case the pressure force must overcome the inward viscous drag, hence the pressure gradient be negative outward. There must be a maximum somewhere in between.

Integration of (16) gives the desired *expression for the pressure* as a function of the distance r from the centre

$$p = \tfrac{3}{2}A \ln\frac{R}{r} - \tfrac{3}{20}B\left(\frac{1}{r^2} - \frac{1}{R^2}\right), \tag{18}$$

if R is the radius at which the outflow is considered to occur evenly in all directions (in our experiments the outflow is really at one point on the edge of the basin). The pressure has been normalised so that it is zero at the outflow.

For an open basin the equation applies equally well for the reasons stated in section 3, and then h is the depth of the liquid, V the surface velocity and R the radius (now of the basin) at which the outflow occurs. Fig. I gives the solution for the case when both coefficients in (18) are unity, viz. $\frac{3}{2}A = 1$, $\frac{3}{20}B = 1$. For water this corresponds to an outflow $Q = 1{\cdot}65$ cm.^{3}/sec. and a depth $h = 0{\cdot}203$ cm., according to (16*a*), (16*b*), which are quantities of the same order as in the actual experiments. (The Q is a little larger than in the experiments, but, as will be pointed out below, the actually measured Q is probably smaller than the Q for the unstable radial solution which should be used in the formulæ.) The maximum pressure, indicated by the circle, is 1·405 dynes/cm.^{2}, hence extremely small; according to (17) it occurs at $r_M = 2$ cm. For larger r the pressure decreases, until at the edge of the basin $R = 9{\cdot}4$ cm. it is zero by assumption. For smaller r the pressure likewise decreases, finally becomes negative, and at $r = 1$ mm., which is of the order of the size of the hole in our experiments, it is $-95{\cdot}5$ dynes/cm.^{2}, or about one millimetre of water. (For lower values of r the curve has been continued on a ten times smaller scale.) The dotted line at large r refers to the logarithmic term and at small r to the inverse square term of (18).

We are now to consider the question of the stability of the radial solution (15) or (16) in a manner analogous to that of section 3. So we again introduce at $t = 0$ a disturbance of radial velocities within a small sector $\Delta\theta$, the disturbed velocity being given by

$$V = \frac{k + \delta k}{r}, \qquad v = \frac{k + \delta k}{r}\left(1 - \frac{z^2}{h^2}\right), \tag{19}$$

so that, also for the disturbed motion, (9) is satisfied.

Since the stream lines of the disturbed motion are parallel to the plates, the hydrodynamical equation of motion is the two-dimensional one (6), with the additional viscosity force per unit volume and unit mass f_μ/ρ on the left-hand side, and since again the sideways velocity is zero, we have for the disturbed motion at $t = 0$

$$\frac{\partial v}{\partial t} = -\frac{1}{\rho}\frac{\partial p}{\partial r} - v\frac{\partial v}{\partial r} + \frac{f_\mu}{\rho}. \tag{20}$$

Using (19), the viscosity force in this equation is given by

$$f_\mu = -\mu\frac{\partial^2 v}{\partial z^2} = -\frac{2\mu(k + \delta k)}{h^2 r}, \tag{21}$$

provided we neglect the viscosity forces in so far as they are due to the difference in radial velocities in adjacent elements $d\theta$ of which $\Delta\theta$ is composed. This is justified, provided that the width $r\Delta\theta$ of the element $\Delta\theta$ is much larger than the depth h, yet we should have $r\Delta\theta$ very much smaller than r. So the depth should really be very small.

Like the case for the undisturbed motion, the approximation is now introduced that (20) holds for the average as regards z. We adopt therefore the equation of motion for the disturbed motion

$$\frac{\partial\bar{v}}{\partial t} = -\frac{1}{\rho}\frac{\partial p}{\partial r} - \frac{\partial}{\partial r}(\tfrac{1}{2}\overline{v^2}) + \frac{f_\mu}{\rho}, \tag{22}$$

where f_μ is given by (21).

Again, because the disturbed sector is very small, we assume that the pressure within this sector approaches the normal undisturbed value prevailing in adjacent regions.* Substituting, for this reason, the undisturbed pressure (15), the disturbed viscosity force (21) and $\overline{v^2}$ (from (9*b*) and (19)), in the equation of motion (22), we obtain the following expression for the change in average velocity immediately subsequent to the disturbance :—

$$\frac{\partial\bar{v}}{\partial t} = \left(\frac{16}{15}\frac{k}{r^3} - 2\frac{\mu}{\rho}\frac{1}{h^2 r}\right)\delta k = \left(\frac{6}{5}\frac{Q}{\pi h r^2} - 3\frac{\mu}{\rho}\frac{1}{h^2}\right)\delta\bar{v}, \tag{23}$$

where, at the last stage, k is expressed in terms of Q by (11), and δk in terms of $\delta\bar{v}$ by (9*a*) and (10) : $\delta\bar{v} = \frac{2}{3}\delta V = \frac{2}{3}\frac{\delta k}{r}$.

With the exception of fig. 9, the motion in all our experiments is outward.† Then, for the radial solution, k (10) and likewise Q (11) is positive. We see then from (22) that $\frac{\partial\bar{v}}{\partial t} = 0$ for a certain *critical radius* given by

$$r_{cr} = 0{\cdot}632\sqrt{\frac{\rho}{\mu}\frac{Qh}{\pi}} = r_M\sqrt{2}, \tag{24}$$

where 0·632 is the numerical value of $\sqrt{2/5}$.

For $r < r_{cr}$, the coefficient of $\delta\bar{v}$ in (23) becomes positive, and $\frac{\partial v}{\partial t}$ has the same sign as $\delta\bar{v}$. The original disturbance results therefore in an immediate reaction further increasing it, and in this sense we shall call the region within r_{cr} an unstable region. Likewise, for $r > r_{cr}$, the coefficient becomes negative,

* As in section 3, we remark that this assumption is not quite a matter of course. A purely hydrodynamical demonstration is desirable.

† In fig. 9 we had water in a basin with large central opening (diameter 1 cm.) closed by a cork. After shaking metal powder on to the surface, the cork was suddenly removed, and the outflow showed the perfectly radial pattern seen in the figure. Since for this case k (10) or Q (11) is negative, the coefficient of $\delta\bar{v}$ in (23) is negative, the $\partial\bar{v}/\partial t$ opposes the disturbance and tends to annihilate it, and the radial solution ought to be stable for the radial type of disturbance considered. So the observed stability of inward radial motion is theoretically understood.

$\frac{\partial v}{\partial t}$ is opposed to $\delta\bar{v}$, tending thus to annihilate the disturbance, and in this sense we shall call the region outside r_{cr} a stable region. The *critical radius* itself is the *boundary between the unstable and the stable region.*

Now, since the unstable region is that where the larger disturbance subsequent to the infinitesimal disturbance $\delta\bar{v}$ sets in, it is reasonable to expect the large deviations from the radial solution within this region, and likewise to expect a roughly radial case to occur in the stable region. In this sense we shall look upon the unstable region within r_{cr} as the highly disturbed region—that is, the region where the streamers occur—and thus r_{cr} is a rough measure of the length of the streamers. (The correct formulation would be that large deviations from radial symmetry occur for r much smaller than r_{cr}, and small deviations for r much larger than r_{cr}.)

Column 8 of Table I contains the calculated length of the streamers r_{cr} from (24) and the observed values of Q and h in Table I. The fact that it is of the same order as the observed length r_s of column 9 is definitely in favour of the theory. There is, however, a large systematic difference : all observed streamers in column 9 are a great deal larger than those calculated in column 8. This may in part be due to the very approximate character of the theory. It is more likely, however, that the difference is due to the fact that we should use for (24) the outflow Q of the unstable radial case. After this unstable state (supposing it realised for a moment) has passed into the stable streamer case, the flow goes outward in some places, inward in others. This fact in itself tends to make the resulting outflow Q smaller. But also it amounts to increased friction, the individual velocities being larger, which results in a still larger drop of the Q. So if we substitute the Q observed for the streamer case in the formula (24), it seems likely that we get too small values for r_{cr}.

Taking the material of columns 8 and 9 for water and glycerine of the various concentrations together, it seems that an outspoken radial case marked by R occurs for an r_{cr} smaller than 1 cm., whereas a streamer case (measured length or an S in column 9) occurs for an r_{cr} larger than 1 cm. The surface tension of these liquids is not much different, around 60 or 70 dynes/cm., as is seen from the first column. To see whether the streamer phenomenon was in any way influenced by surface tension, we made experiments also with two liquids of small surface tension, around 25 dynes/cm., viz. alcohol and turpentine, likewise given in the table. Whereas the observation for turpentine fits in with the others, alcohol seems not to do so, because, although $r_{cr} = 1{\cdot}7$, a good deal larger than 1 cm., yet it definitely shows the radial case in an open basin, as is also seen in fig. 10. So it does seem that surface tension has a definite influence in the sense that large surface tension favours the streamer phenomenon.

At first sight this fact was rather alarming, the more so since no matter how we tried to modify experimental conditions in an open basin we never succeeded in getting the streamer phenomenon for alcohol and turpentine. So it seems indeed that surface tension plays a part for an open basin. Yet the theory based on viscosity must be essentially correct, and the rôle of

the surface tension a subsidiary one, high surface tension ensuring the required radial flow in horizontal direction shortly after the liquid leaves the hole.

The situation seems to be the following. It has been observed for all liquids that at the centre of the basin just above the inflow hole there generally is a little hill of liquid, no doubt due to the initial upward rush. This disturbs the theoretical phenomenon, since it gives an additional negative $\frac{dp}{dr}$, presumably making for stability of the radial solution near the centre, where otherwise it would be very much unstable. Now it seems likely that, besides gravity, surface tension gives the hill its shape. Surface tension acting on a circle of radius r under an angle ϕ with the horizontal direction and in equilibrium with an upward force due to the pressure p would obey the relation $\sin\phi = pr/(2\sigma)$. Taking for water $r = 1$ mm., $p = 100$ dynes/cm.^{2} (fig. I) and $\sigma = 73$, equilibrium would require $\sin\phi \sim 1/15$, which seems a reasonable value—at any rate there is agreement as regards order of magnitude. Now on this picture small surface tension would favour a high hill, $\sin\phi$ being large (indeed for alcohol and turpentine the hill seems more fountain-like than for water; it would be interesting to carry out actual measurements of the height); and it seems that the additional negative $\frac{dp}{dr}$ might well obliterate the normal value of type fig. I for the smaller radii and thus make the radial solution stable throughout. The same thing would also occur at large surface tensions, provided the r_{cr} was small enough, and it seems that it actually occurs for water and glycerine-water mixtures if r_{cr} is smaller than 1 cm. This indeed seems a likely explanation, and so the theory may well be substantially correct.

Nevertheless the explanation of the central hill may not be quite right, and it seems desirable to carry out a further test of the theory by eliminating the surface tension altogether. This is done in the next section.

5. *Further Test of the Theory by Experiments for Various Liquids under Glass.*—To eliminate the surface tension the surface of the liquid was covered with glass. So we really get the case of liquid between two parallel plates to which the theory applies in its purest form.

The open apparatus described in section 2 could easily be adapted for this purpose. This was done as follows. A crystallising basin of a diameter of 14 cm. was mounted in a hole of like size made in a square tin cover so that its bottom was 2·5 cm. below the cover. Cover and inserted basin are seen photographed from above in figs. 11 to 13. This cover could conveniently be made to rest on the upper three adjusting screws of the apparatus which are fixed to the upper experiment basin (see fig. 2), and properly centred by having two of these screws loosely fit into rings soldered on to the cover from below. The glass bottom of the crystallising basin was first made to rest on the bottom of the experiment basin. One of the screws was turned, and when it caught, this was seen by the displacement of the air bubble in the spirit-level placed in the crystallising basin. From there on a certain number of turns was given to the screw, the pitch of which

was 1 mm., and this gave the separation $2h$. Then the other two screws were turned until the bottom of the basin was level again. Above the outflow a semicircular opening was cut in the cover, so that the outflow of diameter 0·5 cm. could be partly or entirely plugged up if desired, but during the actual experiments no plug was used. On the right of the figures the edge of the experiment basin can be seen projecting. The dark displaced circle is the shadow cast by the rim of the crystallising basin.

Fig. 12 shows the experiment with water (for the experimental conditions see Table II). The streamers were made visible by means of gamboge, a yellow water paint. From a tube of paint two concentric rings were squeezed on to the bottom of the crystallising basin. Most clearly seen in the figure are the inward streams made visible by narrow streaks in between and partly beyond the two rings and which are due to the paint being dragged along from the rings by the water. In between the inward streams are the outward streamers going off in directions *a* and *b*. This experiment definitely shows that the streamers for water are not a surface-tension phenomenon.

Fig. 11 shows the experiment with alcohol (see also Table II). To make the streamers visible, a suspension of very fine aluminium powder in the alcohol was made and poured into the experiment basin, with the outflow temporarily plugged up, after which the glass cover was put on. Then the liquid from the pressure basin was released by pulling out a cork in its outflow, and at the same time the outflow of the experiment basin was opened. Whereas we never succeeded in getting them in an open basin, the outward streamers *a*, *b* and *c* under glass are clearly seen in fig. 11, and also whirls separating them. The streamer case of fig. 11 is in marked contrast to the radial case of fig. 10 without cover. This experiment clearly shows that, although the low surface tension prevents their development in an open basin, the streamers required by theory are present in a covered basin where the surface tension is eliminated.

If one were very critically minded, one could object that perhaps by some unknown influence a glass cover might always produce the streamer phenomenon. To test this, an experiment under glass was carried out with glycerine 81 per cent., which on account of its high viscosity should practically always show a predominantly radial flow. The result is shown in fig. 13, which was taken with an exposure of 3 seconds instead of the usual 1·5 second to make the trails longer, since the motion is rather slow. Because of lack of space the photograph is trimmed down a little. It shows a purely radial pattern with no clear indication of separate streamers. Certainly there is no trace of whirls.

For quantitative comparison with theory we may use Table II, which is arranged like Table I, except that the outflow measured is the quantity $2Q'$ in the theory, and the measured separation of cover and bottom the theoretical quantity $2h$. Again, the observed lengths r_s of the streamers in column 9 are of the same order as the calculated lengths r_{cr} in column 8, but larger to about the same extent as in Table I for open basin. The reason of this discrepancy may be the same as mentioned at the conclusion of section 7, that for the theoretical radius one should have used the Q for

TABLE II

Observed Flow of Streamer Type or Radial Type. Glass Cover

For a flow of the streamer type the average length in cm. r_s of the currents is given in the last column. A flow of radial type is marked by R. The physical constants of the substances are given in Table I.

Note that $2h$ represents the height of the liquid and $2Q$ the outflow in cm.^{3}/sec., whereas h and Q should be substituted in the formula (24) for r_{cr}.

1 Substance	2 Phot. or Vis.	3 Diam. Hole cm.	4 Tube T cm.	5 p_0 cm.	6 $2Q$ cm.^{3}/sec.	7 $2h$ cm.	8 Calc. r_{cr} cm.	9 Obs. r_s or R	Remarks
Water	$p(1)$	0·33	22	1·1	3·3	0·4	2·0	4·6	(1) Fig. 12
Alcohol	$p(1)$	0·33	22	0·7	2·9	0·4	1·5	3·6	Fig. 11
	$p(1)$	0·33	22	6·8	6·5	0·4	2·3	4·7	(2)
Glycerine 81 per cent.:	$p(3)$	0·33	40	21·5	7·8	0·4	0·4	R	(3)

(1) The streamers were reproduced and observed visually in several experiments.

(2) Four more films were taken in about the same range of pressure, all clearly showing the streamers.

(3) In the best photograph there is no clear indication of any streamers right up to the central hole.

the unstable radial solution. Glycerine 81 per cent. having a very small h, only 0·4 cm., shows a radial case R.* Altogether the conclusion seems justified that the observations are in approximate agreement with theory.

6. *Prominences. Streamers in View of Condition of Instability. Some further Liquid Models. Excitation by Non-Reversible Compression.*—In this section we shall deal with the general explanation of streamers in prominences as are shown in Lyot's photograph (fig. 1). The phenomenon has been known for a long time, in particular by the fundamental studies of Pettit. We suggest that the prominence streamers are of a similar character to the streamers of liquid in our experiments, and for this it is in the first place desirable to show that conditions actually existing in prominences at the stage of development concerned are favourable for the production of such streamers.

We may first remark that, as far as viscosity goes, it seems likely that the material in prominences would behave like an ideal liquid. If we think of one of the streamer experiments which have been discussed (or one of those which are to follow), carried out with prominence material in the scale of lengths and velocities in prominences, we would have for h and r the order

* The total absence of streamers and whirls quite close to the centre is perhaps a little unexpected theoretically. But this may be due to the fact that for a radius of the order 0·4 cm., the same as the separation of the plates, the flow certainly is not radial and horizontal, since the liquid enters through the hole of 3 mm. in the bottom. The theoretical case of currents going out radially from an axis is experimentally hard to realise.

10,000 km. instead of 1 cm., a factor 10^9, for $\bar{v}$ the order 10 km./sec. instead of 1 cm./sec., a factor 10^6, so for $Q = 2\pi r h \bar{v}$ a factor 10^{24}. On this account then the r_{cr} (24) would become larger by a factor 3×10^{16}, so if in our water experiment it is 5 cm., it would in the solar experiment have the enormous value $1{\cdot}5 \times 10^{12}$ km., and within this radius the radial solution would be unstable. The factor $\frac{\rho}{\mu}$ for gases is of the same order as for water, but even allowing a few factors 10 for ionisation, we would still retain instability. So the conditions in prominences seem to be very favourable for the production of the streamer phenomenon.

It remains to be shown that the motion in prominences, for the state of development concerned, is likely to be of an unstable type. No doubt any prominence originates as an outburst by which gases are thrown upward. But at the stage of development where the streamers occur, the motion on the films seems to be predominantly downward. Such a downward motion, according to Newton *, follows also the upward motion in solar eruptions,

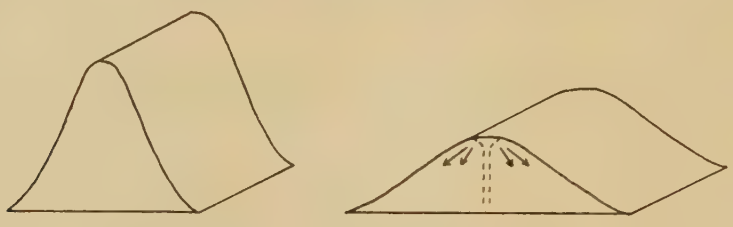

FIG. II.—*Collapse of a ridge of gas.*

which are probably identical with prominences, as Unsöld has pointed out. So it seems reasonable to assume that at this stage there is a general downward rush of gases. It seems also reasonable that at this later stage the original forces of the outburst, whatever their nature, have largely disappeared (compare a volcanic eruption). For the sake of definiteness we may adopt a height of 60,000 km. for the main luminous portion of the prominence, the height of the more extended regions in fig. 1. The study of prominences seen as dark markings in spectroheliograms makes it further likely that they are long structures, as was, *e.g.*, shown in a typical case by Miss M. Roumens.† So we shall assume that in prominences of the streamer type we are dealing with a long ridge of gas which previously has been blown up above the solar surface and now collapses. If the ridge starts at twice its present height, we get the situation schematically represented in fig. II. It starts its downward motion when the height is something like 120,000 km., as is shown on the left. The gases then would go downward, and after a while we would have the situation on the right with a height of 60,000 km. corresponding to the actual prominence in the photograph of fig. 1. As a result of gravity, the upward portion of the ridge would move downward with large velocities and impinge on gases of smaller velocities and higher

* H. W. Newton, *M.N.*, **95**, 650, 1935.

† M. Roumens, *Bull. Soc. As. de France*, **44**, 21, 1929.

pressures. This then seems the condition for which streamers are likely to occur. In fact, the state of motion in the collapsing ridge may roughly be likened to a motion radially outward from a certain axis as considered in section 3, where our proof would hold equally well for outward motion in a sector smaller than 2π.* So though, of course, the motion is not stationary, it seems that the laminar flow on the right-hand side of fig. II is unstable and streamers will occur. We have indicated that by the dotted line representing a streamer, though as yet the actual path of the streamer may be left open.

To approach a little more to the case of fig. II, we have carried out some more experiments. A rectangular basin, $30 \times 17{\cdot}3$ cm., was divided into two portions which communicated from below by a slit 0·8 mm. wide. The largest portion served as a pressure basin into which water was poured to a height of about 1 cm. The smallest portion, $8 \times 17{\cdot}3$ cm., is the experiment basin shown in the photographs of figs. 14 to 16, where the slit is at the top.

In fig. 14 our idea was to realise the top of the long ridge by the slit 17·3 cm. long, and have the liquid go out with large velocity, and then impinge on slower regions. The outflow consisted of four openings of 0·5 cm. seen at the bottom. One indeed sees a strong streamer phenomenon, but the streamers on the surface are alternating. Lower down it was observed that suspended particles all went outward. This model is not quite fair in so far as it does not take into account the divergence of the downward stream in fig. II. So we then took the view of the ridge seen edgewise by narrowing down the slit and plugging up all outflows except the two outer. So the stream should diverge from the slit which is at the top occupying only the central part. Fig. 15 shows the phenomenon for a slit 4 cm. wide from which two divergent streamers are seen to go outward. Fig. 16 shows the same for a slit 2 cm. wide, and here we have only one outward streamer, going off from the centre at the top a little towards the left in the figure. The streamer drawn as an example in fig. II by dotted lines would correspond to this situation.

Summing up the situation, *the downward rush of gases in prominences* of the type considered is *very favourable for the production of streamers*, in the first place, because theoretically the downward diverging laminar motion is likely to be unstable, and in the second place, because in the two-dimensional experimental model of figs. 15 and 16, which roughly represents a perpendicular cross-section of a collapsing ridge of type fig. II, streamers actually are observed. The discussion is greatly simplified, since it was demonstrated that the influence of viscosity on prominence gases must be negligible, and in this respect they behave like an ideal liquid.

The above explanation requires that, like in the liquid experiments, the

* We have remarked in section 3 that outward motion of spherical symmetry divergent from a point is likewise unstable. A sector of this motion would roughly correspond to a collapsing mountain of gas. A finite ridge is intermediate between a mountain and the infinitely long ridge considered in the text, and so may be expected likewise to show the instability.

actual streamers in prominences are moving portions in quieter surroundings of the same material. But on prominence films only the streamers are seen, so that if they occur in a medium of gas, these surrounding gases must be non-luminous. The proposed explanation can therefore only be upheld, if it is made plausible that in a case like fig. 1 only the upper bright portions and the streamers emerging from them are excited, whereas the medium of gas assumed to surround the streamers remains dark ; this calls for a special process of excitation.

Now the very way in which the streamers are assumed to be produced, by the collapsing ridge of fig. II, seems also to provide a suitable way of exciting them by mechanical means. Gurney * has pointed out that material may come down either from the upper chromosphere or from prominences, and that the energy acquired in falling 20,000 km. is more than 2000 volts for calcium, 200 for helium and 50 for hydrogen. According to him, this energy may largely be given up in the form of excitation by inelastic impacts, when the falling material is stopped in lower layers. "The continued existence of prominences and of the upper chromosphere", he remarks, "are matters of observation ; and the continual shower of atoms and ions falling from them seems to be a necessary consequence."

Let us apply this a little more in detail to the situation in fig. II. When the gases come down in the collapsing ridge, they are not falling freely, but are retarded by the pressure force. A good portion of the work done by gravity might thus be transformed into heat or excitation. So in fig. II a free fall over the distance of order 60,000 km. in the figure would produce a velocity of order 180 km./sec., but if the energy goes entirely into heat by adiabatic compression, this would give for hydrogen gas a temperature of $1{\cdot}3 \times 10^6$ °K., so a temperature of order 10^6 °K. is obtained if much of the gravity energy is thus transformed. But since at $1{\cdot}05 \times 10^5$ °K. the thermal energy per atom already equals the ionisation energy 13·5 volts of hydrogen, this high temperature of 10^6 °K. will not be reached, and instead of adiabatic compression one gets excitation and ionisation by inelastic impact, the latter again producing excitation by recombination. In so far therefore as the bulk of matter is retarded, this may be largely in the form of a non-reversible compression, provided the process is quick enough, though of course the temperature may also be quite high. A peculiar feature of this type of excitation is that the exciting agency does not emerge from the photosphere, but is raining down from above. So it is conceivable that one gets the main excited regions well above the solar surface, as is the case for prominences at this stage (see fig. 1).

In order to see whether there is any chance of this process yielding the observed intensity of luminosity, we shall carry out an order of magnitude calculation, using a very much simplified picture. Whereas actually the material is retarded and produces luminosity chiefly in intermediate regions, we shall, for the purpose of calculating the brightness, consider free fall under gravity and sudden stoppage near the solar surface where all the energy is considered to be transformed into excitation. Further, we take

* R. W. Gurney, *M.N.*, **88**, 377, 1928.

the material to be hydrogen, its main constituent, and adopt a concentration N atoms per cm.^{3} independent of the height. The material has started off with the velocity zero, and we examine its state after it has fallen over 60,000 km., this roughly corresponding to the situation in fig. II. Then the energy freed per second and per cm.^{2} cross-section viewed from above is

$$E = \tfrac{1}{2} N m_H v^3, \qquad (25)$$

where m_H is the mass of the hydrogen atom.

On the right-hand side we should substitute $v = 180$ km./sec. required for the free fall over 60,000 km., or $\frac{1}{2} m_H v^3 = 4{\cdot}93 \times 10^{-3}$ erg. cm./sec.

Direct measurements on a rather high and bright prominence by Minnaert and Slob * give for the intensity of emission in $H\alpha$ an equivalent width of the order 10^{-1} A. expressed in the spectral intensity at the centre of the solar disc, or 6×10^5 erg. cm.$^{-2}$ sec.$^{-1}$. The prominence was seen on the limb, and we should have its brightness when viewed from above. In the typical case cited above Miss Roumens derived from the dark marking a width of only 1/20 of the height, so that if the luminosity of the prominence is confined to half the height, the brightness in $H\alpha$ viewed from above may be about 6×10^6. Since $H\alpha$ is presumably largely due to recombination and the not much lower excitation of the third level, the total energy emitted in radiation of all kinds is about 7·2 times the intensity of $H\alpha$ (7·2 = ionisation energy/energy of $H\alpha$), and so we get the observed $E = 4{\cdot}3 \times 10^7$ erg. cm.$^{-2}$ sec.$^{-1}$.

Substituting this on the left-hand side of equation (25) and solving for N, we obtain $N = 9 \times 10^9$ atoms per cm.^{3} as the concentration required for producing the observed luminosity by mechanical excitation. This is only 1/50 of that at the base of the chromosphere, for which Cillié and Menzel † find an electron and ion concentration 4×10^{11} from the intensity of Ba_c, and Pannekoek ‡ 6×10^{11} from the overlapping of the higher Balmer lines by Stark effect. It should be admitted that our considerations are far too simple. But even allowing a good factor on account of this, it seems that *the concentration required for mechanical excitation is by no means excessive*, and that mechanical excitation may well be the main source of luminosity in prominences of the streamer type.

Returning to the question: "Why are the streamers bright and the surrounding gases dark?", it is now possible to give a fairly satisfactory answer. The mechanical excitation takes place from above and so might produce the upper bright regions from which the thin streamers emerge, and the surrounding gases would remain dark.

Another rather mysterious phenomenon which can be elucidated is the extreme thinness of the dark markings in spectroheliograms. In the case cited above Miss Roumens pursued a prominence in absorption (for the K line of Ca^+ and partly for $H\alpha$) as it revolved with the Sun for about

* M. Minnaert and C. Slob, *Proc. Amsterdam Ac.*, **23**, 65, 1930.
† G. G. Cillié and D. H. Menzel, *Harvard Circular*, No. 410, 1935.
‡ A. Pannekoek, *M.N.*, **98**, 709, 1939.

ten days. During several days, 1929 August 25 to September 2, its structure remained roughly the same, having a height of about 80,000 km. The width must have been 3000 to 4000 km., judged by the extreme thinness when viewed edgewise on August 29, and the length about 600,000 km. So one is faced with the apparent difficulty of a long and thin blade of gas standing up above the solar surface and keeping its shape against the action of gravity which in 13 minutes would bring the whole structure down to the solar surface.

A natural way out of the difficulty seems to be offered by the assumption of a collapsing ridge combined with that of mechanical excitation in the following way. We make the not unreasonable assumption that the actual situation in the ridge of gas is like that of fig. 16, consisting then of only one downward stream in fig. II which is marked with dotted lines, and which separates two quieter regions showing opposite whirls. If this is the correct interpretation, and we extend our two-dimensional case to the three-dimensional ridge, then in space we have a downward moving sheet dividing the ridge into two symmetrical halves. The gases made luminous by the non-reversible compression rush downward along this sheet. There then the excitation is strongest, so the second level of H is excited, and the hydrogen will also show in absorption. But also in the sheet the ionisation should be strongest, and so presumably the Ca^+ predominant, whereas outside the sheet there is no direct excitation or ionisation. So also the dark markings of Ca^+ should be thin and approximately of the same shape as for hydrogen, as is actually the case. This then seems to be the *explanation of the extreme thinness of the dark markings in spectroheliograms*. The sheet itself might conceivably break up again into streamers, and so give rise to the thin streamers seen in fig. 1.

It may further be remarked that since the laminar flow is unstable, and so a streamer plane flanked by two whirls is formed, as in fig. 16, the collapse of the ridge is greatly delayed. This might account for the comparative permanence of the structure, although quantitative calculation is necessary.

We have thus far examined only one way of exciting the streamers, but altogether the following three types of excitation seem possible. (1) The material entering the streamers from the more extended regions has a high kinetic temperature and may go on being luminous for a certain length of time during the rapid motion along the streamers. (2) The streamers enter a region of higher pressure, and so, even without the first mechanism, they may become luminous by non-reversible compression as discussed above. Hence it is conceivable that a non-luminous streamer becomes luminous below a certain height, as is observed in the "coronal streamers" of McMath and Pettit.* (3) The knots sticking out beyond a streamer move in a quieter medium of gas and might excite this, and also its own gases, by impact. Since the excitation would be strongest for certain definite velocities corresponding to the excited energy levels, there seems a possibility that an explanation of the discontinuous behaviour of the velocities according to

* R. R. McMath and E. Pettit, *Publ. A.S.P.*, 49, 240, 1937.

Pettit might be found. This, however, requires more careful consideration.

The foregoing makes it likely that conditions in prominences where the material is rushing downward are favourable for producing limited currents either in the form of a sheet or as streamers and that the downward rush is also responsible for the luminosity by mechanical excitation, which, however, is not put forward as the sole mechanism for exciting prominences in general.

Summary.

1. Experiments are discussed in which a flow of liquid spreading out into a basin from a hole in the bottom breaks up into a number of distinct outward currents or streamers. This streamer phenomenon is favoured by small viscosity per unit mass, and more highly viscous liquids tend to produce a purely radial flow.

2. The streamer phenomenon is shown to be due to the fact that for a radial flow of radial symmetry the acceleration is inward and increases with the outward velocity. So, if in a certain sector the velocity is increased, it may be that the force present is unable to keep back sufficiently the liquid in its new state, and the outward motion increases still further. Thus a number of outward streamers result.

3. This condition of instability is worked out quantitatively, and an approximate formula for the length of the currents derived. Experiments with various liquids are discussed, and there is approximate agreement with theory in all cases where the theoretical conditions are fulfilled.

4. The considerations of instability are then applied to streamers in prominences, which occur when there is a general downward rush of gases.

The conception of prominences of the streamer type as a collapsing ridge of gas is discussed, and it is shown that conditions are then favourable for the production of streamers. A water model suggests that the actual motion may take place in the form of a thin sheet dividing this ridge in half and possibly breaking up into streamers.

Following up Gurney's earlier work, it is further shown that the luminosity in such prominences is very likely due to a mechanical excitation consisting of a non-reversible compression of the downward-going gases. This mechanism requires a concentration of the oncoming gases which is not excessive.

In the downward rushing sheet, gases would both be strongly excited and strongly ionised by mechanical excitation. This offers an explanation for the extreme thinness of prominences seen in absorption in $H\alpha$ or Ca^{+} spectroheliograms.

It seems that streamers can be excited in three ways: by high kinetic temperature, by irreversible compression and by collisions with the surrounding gases.

The author gratefully acknowledges his indebtedness to Professor H. H. Plaskett, Director of the University Observatory at Oxford, for his advice and active help throughout the investigation, in particular for the photographic arrangement which is entirely due to him. The author's attention was first called to the astrophysical problem by Sir Arthur Eddington, and discussions with Dr. B. Lyot and Dr. L. d'Azumbuja at the Observatory in Meudon greatly clarified his ideas. Criticism and suggestions were offered by Professor E. A. Milne and Professor W. H. McCrea, who suggested the use of the hydrodynamical equations of motion in the proof of instability. To them the author wishes to express his sincere thanks, as well as to Mr. G. R. Neale for constructing the apparatus and to Miss E. Bellamy for suggesting the use of bronze powder.

University Observatory,
Oxford:
1939 *February*.

STELLAR KINEMATICS AND MEAN PARALLAXES

(Second Paper)

Frank K. Edmondson

(Communicated by Dr. H. Shapley)

Introduction

1. Valuable material regarding the proper motions of faint stars has been obtained at the McCormick Observatory by van de Kamp and Vyssotsky.* In their discussion of this material, these authors have called attention to the unexpectedly large secular parallaxes near the galactic plane, an apparent north-south asymmetry of secular parallaxes with respect to the galactic plane, and systematic differences between mean parallaxes derived from secular parallaxes and tau-components.

van de Kamp and Vyssotsky have also derived relative secular parallaxes of stars from the 9th to the 15th magnitude from the proper motions of the Radcliffe Catalogue. In order to convert these to absolute values, the zero-point at the 10th magnitude was established by means of proper motions in right ascension of the reference stars used at Allegheny, Johannesburg and McCormick in the process of determining the trigonometric parallaxes of Boss stars. A mean correction of $-0^{m}.5$ was applied to the photographic magnitudes in order to reduce them to photovisual magnitudes. The results appear to confirm the discussion of the McCormick material.

2. Mean parallaxes have also been derived from the Radcliffe proper motions by van Hoof † and Oort ‡. van Hoof discussed tau-components in the conventional way, while Oort discussed components chosen in such a way that they contain only a small part of the solar motion and point as closely as possible toward the principal vertex. Similar results were obtained by both methods.

Oort has criticised the McCormick mean parallaxes because they are not confirmed by his discussion of the Radcliffe material. This criticism neglects the fact that the McCormick discussion is based chiefly on secular parallaxes, whereas the discussions by Oort and van Hoof are based on a different component of proper motion. The McCormick observers found systematic differences between π_τ and π_v from their own material, and the calculations of Oort and van Hoof and of van de Kamp and Vyssotsky show that systematic differences also exist between the Radcliffe π_τ and π_v.

3. The interpretation of the McCormick results in terms of mean

* van de Kamp and Vyssotsky: "A Study of the Proper Motions of 18,000 Stars," *McCormick Publications*, Vol. VII (1937), or *A.J.*, 1054, 1055, 1058, 1059, (1937, 1938).

† van Hoof, *B.A.N.*, 289, 1936.

‡ Oort, *B.A.N.*, 290, 1936.

parallaxes has been criticised effectively by van Rhijn * and Oort.† These authors have shown that the McCormick mean parallaxes are not in accord with what is known about stellar distribution as derived from star counts.

The relationship of the mean parallaxes to star counts can also be studied by means of an extension of the numerical analysis developed by Bok. ‡ The result of such an analysis is to show that it is possible to represent the McCormick mean parallaxes equally well by (1) an absorption of the order

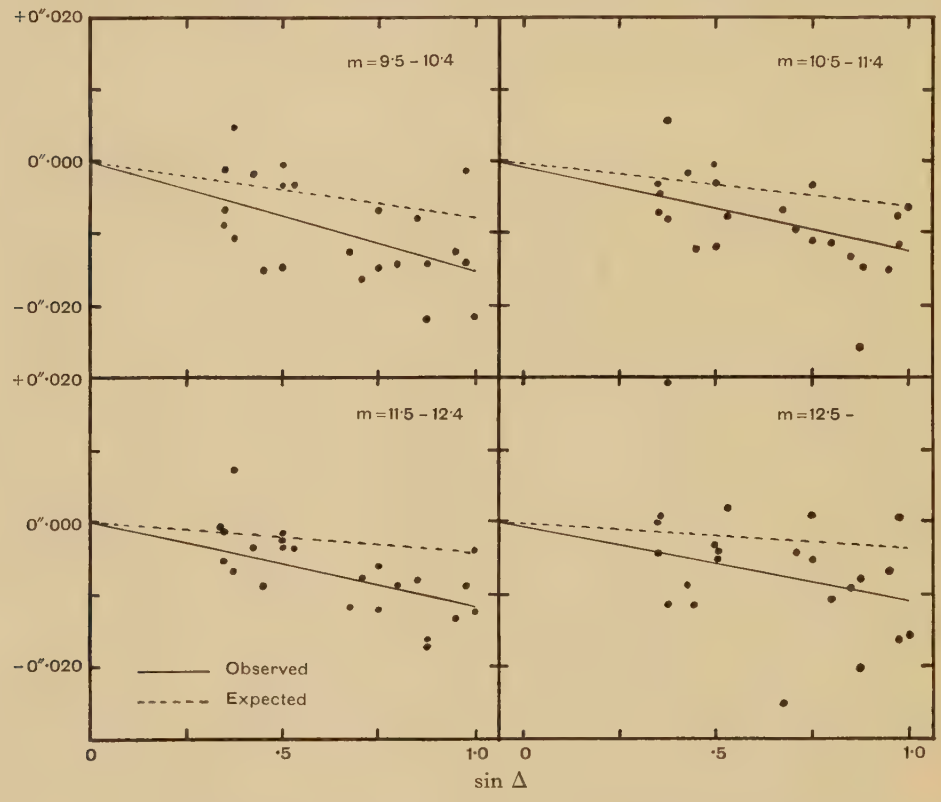

FIG. 1.—*Mean v-component (counted positive toward the apex) plotted against sin Δ (Δ = distance from the solar apex). The heavy line corresponds to the value given by van de Kamp and Vyssotsky, and the dotted line corresponds to the star count value given in Table 1b.*

of two photovisual magnitudes per kiloparsec (the result obtained by van de Kamp and Vyssotsky), or (2) a very rapid density decrease with distance from the Sun in the galactic plane. Neither of these results is in harmony with star count data.

It has been known for many years that an analysis of star counts cannot separate the effects of absorption and density decrease. We wish to emphasize, similarly, that an analysis of mean parallaxes cannot separate the

* van Rhijn, *G.P.*, 47, 1936.
† Oort, *B.A.N.*, 290, 1936.
‡ Bok, *H.C.*, 371, 1931.

effects of absorption and density decrease. One can obtain any absorption coefficient that he wishes by properly choosing the density law, and we must conclude that the two magnitudes per kiloparsec obtained by van de Kamp and Vyssotsky is entirely due to their rather arbitrary assumptions about the density law.

4. The inconsistency between the McCormick mean parallaxes and star counts is of fundamental significance, and requires explanation. The simplest explanation is to lay the blame on systematic and accidental errors of the proper motions. Indeed, Oort remarks *: "In my opinion the deviating McCormick results are probably due to systematic errors in the proper motions and to the too large number of unknowns introduced by the authors." Furthermore, fig. 1 shows that the scatter of the observations is large enough to throw doubt on the reality of the inconsistency. Still, it is of interest to examine the possibility of interpreting the effect, assuming for the moment that it is real. The discussion will be confined to stars in low galactic latitudes in order to reduce the number of unknowns to a minimum.

The Possibility of a Change of the Luminosity Function

5. It should be possible to reconcile the McCormick mean parallaxes with star counts by modifying the luminosity function. Qualitatively, the reasoning is as follows: The fundamental fact of observation is that the McCormick mean parallaxes of faint stars in low galactic latitudes are much larger than they should be if previous work on the brighter stars is correct. If we visualize the problem in terms of an (m, $\log \pi$) table, we see that the influence of the absolutely bright stars in distant shells must be removed (either by absorption or density decrease) in order to represent the mean parallaxes. Then in order to represent the star counts, it will be necessary to add a very large number of stars to the nearby shells. These stars will be fainter than $M = +3$. The largest increase (a factor of 10 or more) will be for stars fainter than $M = +5$, or for stars of spectral class Go and later.

6. Such a drastic modification of the luminosity function must find support from other types of observations before it can be accepted. At the present time, such support seems to be lacking. van Maanen's luminosity curve for stars of large proper motion † agrees with van Rhijn ‡ at $M = +6$, and gives only three times as many stars at $M = +10$. This would not affect either mean parallaxes or star counts to any appreciable extent.

Stronger evidence against a drastic change of the van Rhijn luminosity function is provided by Luyten's recent work. § Luyten's luminosity function is in essential agreement with van Rhijn over the range common to both of them, and reaches a maximum at $M = +14{\cdot}7$ photographic. Thus, a large change in the photovisual luminosity function seems to be ruled out also.

* Oort, *B.A.N.*, 290, 1936.
† van Maanen, *Ap. J.*, **85**, 26–39, 1937, or *Mt. Wilson Contr.*, 562.
‡ van Rhijn, *G.P.*, 47, 1936.
§ Luyten, *M.N.*, **98**, 677–680, 1938.

The Possibility of a Second Order Galactic Rotation Effect

7. Before the details of the work by van de Kamp and Vyssotsky were available, the possibility of explaining their results * by a second order galactic rotation effect suggested itself. The formulæ showing the effect of second order galactic rotation terms on tau- and upsilon-components have already been published in a previous paper.†

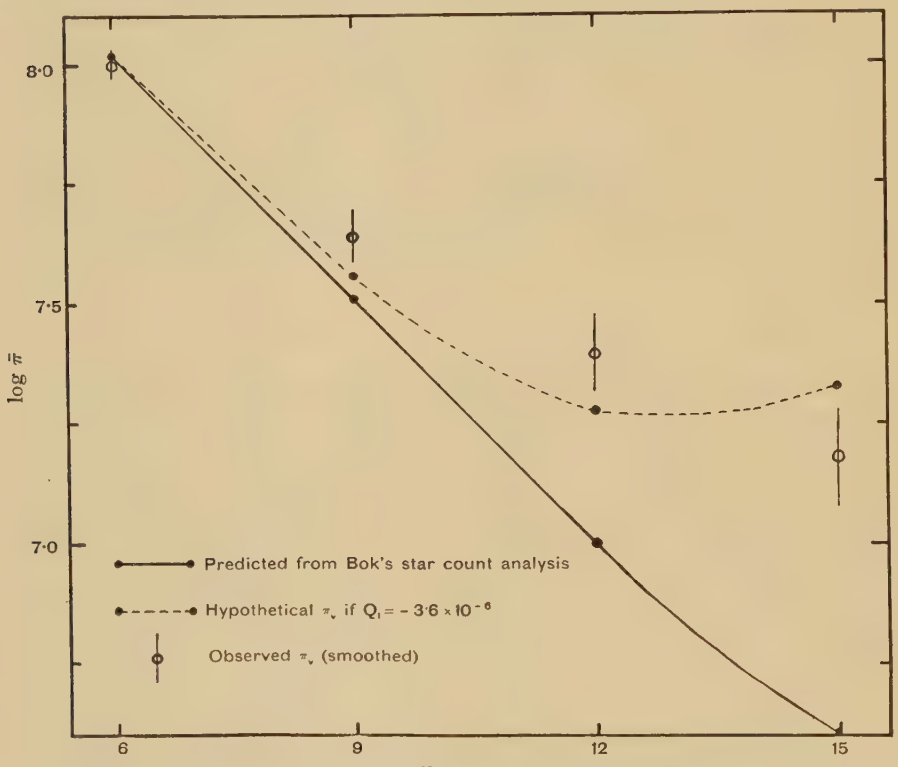

FIG. 2.

The formula for π_v in terms of the true mean parallax $\bar{\pi}$ is

$$\pi_v = \bar{\pi} + \frac{Q_1}{V_0}\frac{f(\beta)K(\beta)}{\bar{\pi}}.$$

V_0 is the velocity of the Sun relative to the nearby stars, and Q_1 is defined by

$$Q_1 = \frac{1}{8}\left[\frac{d^2\bar{M}}{dR^2} + \frac{1}{R}\frac{d\bar{M}}{dR} - \frac{\bar{M}}{R^2}\right] = \frac{1}{8}\left[\frac{d^2\bar{M}}{dR^2} - 3{\cdot}10^{-6}\right],$$

where $\bar{M}$ is the mean velocity of galactic rotation at the Sun's distance R from the galactic centre. $K(\beta)$ is the product of mean parallax and mean distance $\bar{\pi} \cdot \bar{r}$, and is always greater than unity. $f(\beta)$ is equal to $-2{\cdot}20$, if

* van de Kamp and Vyssotsky, *P.N.A.S.*, **21**, 419–428, 1935; *P.A.A.S.*, **8**, 226–227, 1935.

† Edmondson, *M.N.*, **97**, 473–485, 1937, or *Harvard Reprint*, 138.

$\beta = 0°$ and the co-ordinates of the apex are taken equal to the values used by van de Kamp and Vyssotsky.

8. If we can estimate the value of the true mean parallax $\bar{\pi}$ from star count data, it will be possible to use the McCormick π_v to find the order of magnitude of Q_1. The following procedure, which is admittedly crude, has been followed for lack of anything better. The density law was assumed to be a smoothed representation of the result found by Bok * for the mean distribution in low galactic latitudes, and the corresponding photovisual absorption coefficient was assumed to be two-thirds of the photographic absorption coefficient used by Bok in the derivation of the density law. van Rhijn's visual luminosity function † was adopted, and values of $\bar{\pi}$ and $K(\beta)$ were computed by numerical integration for magnitudes 6, 9, 12, and 15. Smoothed values of π_v for these same four magnitudes were derived from the McCormick discussion. The adopted values of $\bar{\pi} \cdot \bar{r}$ and $\bar{\pi}$ corresponding to Bok's solutions for $\Delta m = 0{\cdot}00$, $0{\cdot}40$ and $0{\cdot}80$ and the adopted values of π_v are given in Tables I*a*, I*b* and I*c*.

The best representation of the secular parallaxes is obtained when we put

$$Q_1 = -2{\cdot}7 \cdot 10^{-6},\ -3{\cdot}6 \cdot 10^{-6} \text{ and } -4{\cdot}5 \cdot 10^{-6}$$

or

$$\frac{d^2\bar{M}}{dR^2} = -1{\cdot}9 \cdot 10^{-5},\ -2{\cdot}6 \cdot 10^{-5} \text{ and } -3{\cdot}3 \cdot 10^{-5}$$

respectively in Tables I*a*, I*b* and I*c*. The computed values of π_v and the residuals are given in the last two columns of these tables. Fig. 2 is a graphical representation of Table I*b*. It is clear that we have here a possible way to explain the McCormick observations.

TABLE I*a*

Unit $= 0''{\cdot}001$

Magnitude	$\bar{\pi} \cdot \bar{r}$	$\bar{\pi}$	McCormick π_v	Computed π_v	O − C
6	2·8	10·7	10·0	10·8	−0·8
9	3·2	3·6	4·4	3·9	+0·5
12	2·8	1·3	2·5	1·9	+0·6
15	2·3	0·4	1·5:	2·1	−0·6

TABLE I*b*

Unit $= 0''{\cdot}001$

Magnitude	$\bar{\pi} \cdot \bar{r}$	$\bar{\pi}$	McCormick π_v	Computed π_v	O − C
6	2·5	10·4	10·0	10·5	−0·5
9	2·8	3·2	4·4	3·6	+0·8
12	2·2	1·0	2·5	1·9	+0·6
15	1·8	0·4	1·5:	2·2	−0·7

* Bok, *H.C.*, 371, 1931, Table XI. † van Rhijn, *G.P.*, 47, 1936.

TABLE I*c*

Unit = 0″·001

Magnitude	$\bar{\pi} \cdot \bar{r}$	$\bar{\pi}$	McCormick π_v	Computed π_v	O − C
6	2·5	9·3	10·0	9·4	+0·6
9	2·6	3·0	4·4	3·4	+1·0
12	1·7	1·0	2·5	1·9	+0·6
15	1·4	0·5	1·5 :	2·0	−0·5

9. The existence of this effect can be checked by means of the tau-components. If the effect exists, the mean tau-component will not be zero everywhere, but will vary systematically depending on the position in the sky. In general,

$$T_{\lambda\beta} = \frac{rQ_1}{4{\cdot}74} \cdot F(\lambda, \beta, L, B).$$

F is the trigonometrical part of the formula at the top of page 479 in the paper in *M.N.*, 97.

Fig. 3 shows the observed mean tau-components derived from the McCormick data * plotted against the function F. The heavy line shows the least squares fit (forced to pass through the origin, of course), and the dotted line shows the relationship expected on the basis of the upsilon-component result corresponding to Table I*b*. The expected results corresponding to Tables I*a* and I*c* are hardly distinguishable from this on the scale of these diagrams.

The consistency of sign and order of magnitude of the effect as derived from four different magnitude groups is distinctly encouraging, despite the scatter of the individual points. The ratio of the least squares value of $\frac{rQ_1}{4{\cdot}74}$ to its mean error is 2·1, 2·4, 2·1 and 1·0 for the four groups.

The mean value of Q_1 derived from the tau-components for all four magnitude groups together is

$$-5{\cdot}3 \cdot 10^{-6}, \quad -5{\cdot}3 \cdot 10^{-6} \text{ or } -5{\cdot}6 \cdot 10^{-6},$$

corresponding to Tables I*a*, I*b* and I*c* respectively. The mean error is

$$\pm 1{\cdot}3 \cdot 10^{-6}, \pm 1{\cdot}3 \cdot 10^{-6} \text{ or } \pm 1{\cdot}6 \cdot 10^{-6},$$

so that the ratio of Q_1 to its mean error is 4·1, 4·1 or 3·5.

10. There is still one apparent inconsistency that requires explanation.

* Derived from the mean motions in Tables 11.2 and 11.3 of *McCormick Publications*, vol. vii. The Oort term

$$0''{\cdot}003 \cos 2(l - l_0) - 0''{\cdot}003$$

was subtracted from the observed values of $(\mu_\lambda \cos b)$.

The formula for π_τ in terms of the true mean parallax $\bar{\pi}$ is

$$\pi_\tau = k \,.\, \bar{\pi}.$$

The formula for k can be found on page 479 of the paper in *M.N.*, **97**.

From the McCormick data and the values derived for Q_1, we find that k should be about 1·05 for stars of the 12th magnitude. For the brighter

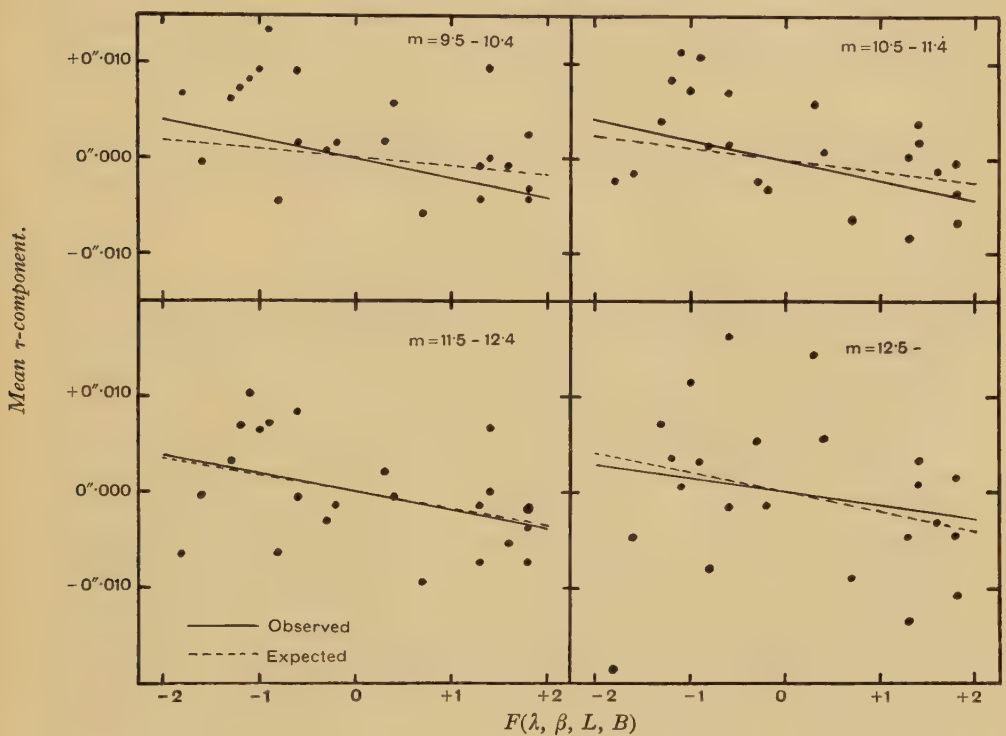

FIG. 3.

stars, k will be smaller than 1·05. Hence, we should expect to find the McCormick π_τ nearly equal to the computed values of $\bar{\pi}$. Instead of this, the given values of π_τ are much larger than the computed values of $\bar{\pi}$. In

TABLE II

Accidental Errors of the McCormick Motions (*unit* = 0″·001)

m	McCormick	Revised	Difference
8·76	7·0	8·8	1·8
10·04	5·5	7·4	1·9
11·02	5·5	7·8	2·3
11·94	6·5	8·2	1·7
12·72	8·0	9·5	1·5

fact, they are in better agreement with the given values of π_v. This can be accounted for if we assume that the accidental errors of the McCormick proper motions have been slightly underestimated. Table II gives the probable errors that were adopted by van de Kamp and Vyssotsky and the probable errors that will reconcile the π_τ with the $\bar{\pi}$.

Effect on Radial Velocities

11. The formula for radial velocity (corrected for local solar motion) is

$$r^2Q_1 \sin \lambda + rA \sin 2\lambda + r^2Q_2 \sin 3\lambda,$$

for stars in the galactic plane. We have (approximately)

$$Q_1 = -4{\cdot}5 \cdot 10^{-6}$$

and

$$Q_2 = Q_1 + 1{\cdot}5 \cdot 10^{-6} = -3{\cdot}0 \cdot 10^{-6}.$$

Hence, for stars 1000 parsecs from the Sun we should expect to find a term in $\sin \lambda$ with a coefficient of $-4{\cdot}5$ km./sec., and a term in $\sin 3\lambda$ with a coefficient of $-3{\cdot}0$ km./sec. Since this effect varies as the square of the distance, these coefficients will only be $-1{\cdot}1$ km./sec. and $-0{\cdot}8$ km./sec. for stars at a distance of 500 parsecs.

Unfortunately, existing determinations of radial velocity cannot be used to check this effect, since the value of Q_1 derived from the McCormick proper motions applies strictly to stars grouped according to apparent magnitude. There is no reason to expect special groups of objects (O and B stars, Cepheids, etc.) to show the same behaviour as stars classified according to apparent magnitude. Hence, radial velocities of 11th and 12th magnitude stars in low galactic latitudes are needed to check the proper motion result. The expected amplitudes of the first and third harmonic terms for 12th magnitude stars are -15 km./sec. and -10 km./sec. Such an effect should be observable, despite the possible influence of variations in interstellar absorption as a function of galactic longitude as pointed out in the paper in *M.N.*, **97**.

Significance of these Results

12. Studies of the radial velocities of globular clusters * and planetary nebulæ † have shown that the circular velocity in the galaxy is approximately constant over a large range of distances. In the latter case, the circular velocity is 259, 275 and 279 km./sec. at distances of 5, 10 and 15 kiloparsecs from the galactic centre.

The value of Q_1 derived from the McCormick data indicates a mean rotational velocity of 210, 275 and 210 km./sec. at distances of 8, 10 and 12 kiloparsecs from the galactic centre. Similar differences between circular velocity and the mean rotational velocity of groups of stars have been observed in the neighbourhood of the Sun.‡ The stars that show this effect are known

* Edmondson, *A.J.*, 1036, 1935. Reprinted as *Lowell Obs. Bulletin*, 88.
† Berman, *L.O.B.*, 486, 1937.
‡ *E.g.* Stromberg, *Ap. J.*, **61**, 363–388, 1925, or *Mt. Wilson Contr.*, 293.

as "high velocity stars," because of their high velocities relative to the Sun. These high relative velocities and corresponding small rotational velocities are due to deviations from circular motion.

The large value of Q_1, if real, must be interpreted to mean that the percentage of high velocity stars varies with distance from the galactic centre and reaches a minimum in the neighbourhood of the Sun. In other words, circular motions are more stable in the neighbourhood of the Sun than in adjacent regions toward and away from the galactic centre. If this proves to be true, it should have important theoretical consequences.

I wish to thank all of those who have read the preliminary drafts of this paper for helpful advice and criticism. I am particularly indebted to Dr. Bok, Dr. Greenstein, Dr. McCuskey, and Dr. Kuiper.

Summary

1. The mean parallaxes in the 0°–10° galactic zone which have been determined at the McCormick Observatory by van de Kamp and Vyssotsky are not consistent with star counts. It is possible that the inconsistency is due to the systematic and accidental errors of the proper motions, but it seems desirable to examine the possibility of other explanations.

2. The possibility of a change of the luminosity function is examined and ruled out.

3. The possibility of a second order galactic rotation effect is examined. Such an effect seems to exist in both the tau- and the upsilon-components, although it is nearly at the limit of statistical significance. Some confidence in the reality of the effect should be inspired by the consistent values of the second order coefficient derived independently from both components of proper motion.

4. The existence of the second order terms can be checked by observing radial velocities of faint stars in low latitudes. At the 12th magnitude, first and third harmonics are expected with amplitudes of −15 and −10 km./sec.

5. The significance of a second order effect of the observed size is discussed.

Kirkwood Observatory,
Indiana University,
Bloomington, Indiana:
December 1938.

THE DISTRIBUTION OF THE POSITION ANGLES OF THE EXTRA-GALACTIC NEBULÆ IN HOROLOGIUM

F. G. Brown

The catalogue of 7889 galaxies in Horologium * covers an area of less than 200 square degrees which is exceptionally rich in small nebulæ. It contains 355 objects sufficiently large and elongated for the position angles, which the major axes make with the meridian, to be estimated with reasonable accuracy.

These position angles have been classified to the nearest 10° and the results are given in the table.

Classification of Galaxies in Horologium according to the Position Angle of the Major Axis

P.A.	0°	10°	20°	30°	40°	50°	60°	70°	80°
No. of galaxies	20	25	36	35	47	29	25	24	14
P.A.	90°	100°	110°	120°	130°	140°	150°	160°	170°
No. of galaxies	11	9	10	13	8	12	14	11	12

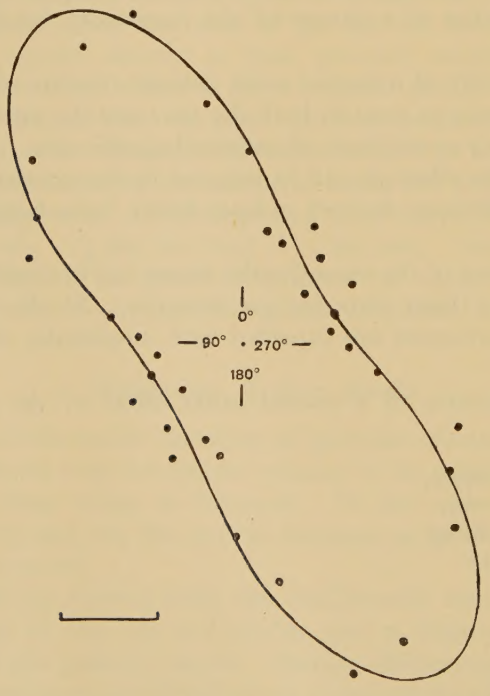

DIAGRAM.—*Frequency of occurrence of all known position angles among the galaxies of the Horologium region, showing the large excess about 33°. The linear scale corresponds to a frequency of one position angle to every degree.*

* *H.A.*, 88, No. 5.

A smoothed curve giving the relative frequencies for all position angles is reproduced in the annexed diagram, the values for angles between 0° to 180° being duplicated between 180° and 360° to close the curve. The figure shows a fourfold extension in the direction of 33° compared with the direction at right angles to this.

The marked preference for certain position angles is also shown by the nebulæ in other regions. Thus, the elongated galaxies between 2 hours and 4 hours right ascension and −15° and +40° declination reveal a nearly threefold preference for values about 20° while the small nebulæ (under 1′ diameter) in the Coma Virgo area show a similar threefold concentration around position angle 80°.

Whether these preferences are indications of a general structure in the extra galactic field, or merely evidence of local peculiarities, may only be decided when further lists of position angles are available, and it is hoped that these will not be long delayed.

Summary

Position angles of elongated galaxies in the Horologium region show a fourfold preference for values round about 33° over the direction at right angles to this.

Other less well-observed regions appear to show similar preferential distributions of the position angles.

Vale House, Park Road,
Forest Hill, S.E. 23 :
1939 *April.*

Errata

M.N., **99**, 175 (W. M. Smart, The Moving Cluster in Taurus) :—

Line 19 : *For* "58·9" and "−3·8" *read* "25·1" and "15·6."
Line 20 : *For* "59·0" and "R.A. 90°, Dec. −3°·7," *read* "29·6" and "R.A. 93°, Dec. +32°."
Line 21 : *For* "172°" and "−7°," *read* "148°" and "+9°."